

# Dark matter and flavor anomalies in the light of vector-like fermions and scalar leptoquark

Suchismita Sahoo<sup>a,1,\*</sup> Shivaramakrishna Singirala<sup>b,1,†</sup> and Rukmani Mohanta<sup>b1,‡</sup>

<sup>1a</sup>*Department of Physics, Central University of Karnataka, Kalaburagi-585367, India*

<sup>b</sup>*School of Physics, University of Hyderabad, Hyderabad-500046, India*

## Abstract

We make a comprehensive study of vector-like fermionic dark matter and flavor anomalies in a simple extension of standard model. The model is added with doublet vector-like fermions of quark and lepton types, and also a  $S_1(\mathbf{\bar{3}}, \mathbf{1}, 1/3)$  scalar leptoquark. An additional lepton type singlet fermion is included, whose admixture with vector-like lepton doublet plays the role of dark matter and is examined in relic density and direct detection perspective. Electroweak precision observables are computed to put constraint on model parameter space. We constrain the new couplings from the branching ratios and angular observables associated with  $b \rightarrow sll(\nu_l\bar{\nu}_l)$ ,  $b \rightarrow s\gamma$  decays and also from the recent measurement on muon anomalous magnetic moment. We then estimate the branching ratios of the rare lepton flavor violating  $B_{(s)}$  decay modes such as  $B_{(s)} \rightarrow l_i^\mp l_j^\pm$ ,  $B_{(s)} \rightarrow (K^{(*)}, \phi)l_i^\mp l_j^\pm$ .

---

\*Electronic address: suchismita8792@gmail.com

†Electronic address: krishnas542@gmail.com

‡Electronic address: rmsp@uohyd.ernet.in

## I. INTRODUCTION

The well established fundamental theory of particle physics, Standard Model (SM), failed to explain the matter-antimatter asymmetry, existence of dark matter and the observation of tiny neutrino mass, which provide a clear indication of the presence of new physics (NP) beyond it. After the phenomenal discovery of the Higgs boson, though the LHC experiment has not directly observed any new heavy particles beyond the SM, indirect searches through rare decays of bottom hadrons have provided several intriguing hints of NP. In the last few years, a collection of interesting deviations from the SM have been manifested in various angular observables associated with flavor changing neutral current (FCNC)  $b \rightarrow sl^+l^-$  [1–4] and flavor changing charge current (FCCC)  $b \rightarrow c\tau\bar{\nu}_\tau$  [5–16] decay modes. Most relevant anomalies include the lepton flavor universality violating (LFUV) parameters such as  $R_K$  ( $2.5\sigma$  deviation) [1, 2, 17–19],  $R_{K^*}$  ( $2.2\sigma - 2.4\sigma$  deviation) [3, 20],  $R_{D^{(*)}}$  ( $3.08\sigma$  deviation) [21–24],  $R_{J/\psi}$  ( $2\sigma$  deviation) [10, 25, 26] in which the hadronic uncertainties cancelled out significantly. The precise analysis of these deviations are needed in both the SM and beyond the SM scenarios in order to probe the structure of NP.

The hypothetical color triplet bosonic particle, leptoquark arises naturally from the unification of quarks and leptons and its existence can be found in many extended SM theories [27–38]. The scalar (spin = 0) or vector (spin = 1) leptoquarks carry both the lepton and baryon quantum numbers. Scenarios with such particles ease to address the flavor anomalies, already investigated in literature [19, 39–70]. In the present context, we use a  $S_1(\bar{\mathbf{3}}, \mathbf{1}, 1/3)$  scalar leptoquark to obtain NP contribution to the above quoted anomalies in flavor sector. On the other hand, vector-like fermions are well motivated in low energy scenarios, for review, please see [71] and references therein. We consider vector-like fermions of both quark and lepton type, with SM hypercharge assignment. The neutral component of the vector-like lepton can explain the observed relic density of DM in the Universe [72]. To avoid  $Z$ -portal direct detection cross section violating the existing spin-independent limits, a trick of mixing with an vector-like singlet lepton is applied in so called singlet-doublet scenarios. Such models are well contained in literature [73–90].

The paper is structured as follows. Section-II provides the particle content, relevant interaction Lagrangian and also the mixing in neutral vector-like lepton sector. Section-III is presented with the relic density of DM with contributions from annihilations and co-

annihilations in various allowed portals. Further, detection prospects are also addressed. Electroweak precision constraints on the model parameters are discussed in section-IV. Section-V discusses the constraints from the quark sector and also from muon anomalous magnetic moment. The implication of new constrained parameters on the lepton flavor violating  $B_{(s)}$  decay modes are presented in section-VI. Brief comments on neutrino mass are given in section-VII. Finally, the conclusive remarks are provided in section-VIII.

## II. NEW MODEL WITH LEPTOQUARKS

We extend SM with vector-like fermion multiplets, one doublet of quark type ( $\psi_q$ ), one doublet of lepton type ( $\psi_\ell$ ) and also a lepton singlet ( $\chi_\ell$ ). The model also includes a  $(\bar{\mathbf{3}}, 1, 1/3)$  scalar leptoquark (SLQ) and the new particles are assumed to be odd under a discrete  $Z_2$  symmetry. The particle content of the model and their quantum numbers are displayed in Table I.

TABLE I: Fields and their charges in the present model.

	Field	$SU(3)_C \times SU(2)_L \times U(1)_Y$	$Z_2$
Fermions	$Q_L \equiv (u, d)_L^T$	$(\mathbf{3}, \mathbf{2}, 1/6)$	+
	$u_R$	$(\mathbf{3}, \mathbf{1}, 2/3)$	+
	$d_R$	$(\mathbf{3}, \mathbf{1}, -1/3)$	+
	$\ell_L \equiv (\nu, e)_L^T$	$(\mathbf{1}, \mathbf{2}, -1/2)$	+
	$e_R$	$(\mathbf{1}, \mathbf{1}, -1)$	+
Vector-like fermions	$\psi_q \equiv (\psi_u, \psi_d)^T$	$(\mathbf{3}, \mathbf{2}, 1/6)$	-
	$\psi_\ell \equiv (\psi_\nu, \psi_l)^T$	$(\mathbf{1}, \mathbf{2}, -1/2)$	-
	$\chi_\ell$	$(\mathbf{1}, \mathbf{1}, 0)$	-
Scalars	$H$	$(\mathbf{1}, \mathbf{2}, 1/2)$	+
	$S_1$	$(\bar{\mathbf{3}}, \mathbf{1}, 1/3)$	-

The relevant interaction terms emerging from the Lagrangian are given as

$$\begin{aligned}
\mathcal{L} = & -y_\ell \overline{Q_L^C} S_1 \epsilon^{ab} \psi_{\ell L} - y'_\ell \overline{d_R^C} S_1 \chi_{\ell R} - y_q \overline{\psi_{qL}^C} S_1 \epsilon^{ab} \ell_L - y'_q \overline{Q_L^C} S_1^* \epsilon^{ab} \psi_{qL} - y_D \overline{\psi_\ell} \tilde{H} \chi_\ell + \text{h.c.} \\
& - M_q \overline{\psi_q} \psi_q - M_\psi \overline{\psi_\ell} \psi_\ell - M_\chi \overline{\chi_\ell} \chi_\ell + \overline{\psi_\ell} \gamma^\mu \left( i\partial_\mu - \frac{g}{2} \boldsymbol{\tau}^a \cdot \mathbf{W}_\mu^a + \frac{g'}{2} B_\mu \right) \psi_\ell + \overline{\chi_\ell} \gamma^\mu (i\partial_\mu) \chi_\ell \\
& + \overline{\psi_q} \gamma^\mu \left( i\partial_\mu - \frac{g}{2} \boldsymbol{\tau}^a \cdot \mathbf{W}_\mu^a - \frac{g'}{6} B_\mu \right) \psi_q + \left| \left( i\partial_\mu - \frac{g'}{3} B_\mu \right) S_1 \right|^2, \tag{1}
\end{aligned}$$

and the scalar potential of the model is

$$V(H, S_1) = \mu_H^2 H^\dagger H + \lambda_H (H^\dagger H)^2 + \mu_S^2 (S_1^\dagger S_1) + \lambda_S (S_1^\dagger S_1)^2 + \lambda_{HS} (H_2^\dagger H) (S_1^\dagger S_1).$$

### A. Neutral fermion mass spectrum

Due to the presence of Dirac term between the lepton multiplets and Higgs in eq. (1), the new neutral fermions mix among themselves and the corresponding mixing matrix takes the form

$$M_N = \begin{pmatrix} M_{\psi_\ell} & M_D \\ M_D & M_{\chi_\ell} \end{pmatrix}, \quad \text{where} \quad M_D = \frac{2y_D v}{\sqrt{2}}. \tag{2}$$

One can diagonalize the above mass matrix using a unitary matrix  $U_\alpha = \begin{pmatrix} \cos \alpha & -\sin \alpha \\ \sin \alpha & \cos \alpha \end{pmatrix}$  as  $U_\alpha^T M_N U_\alpha = \text{diag}(M_{N_1}, M_{N_2})$ , with  $\alpha = \frac{1}{2} \tan^{-1} \left( \frac{2M_D}{M_{\psi_\ell} - M_{\chi_\ell}} \right)$ . The relation between flavor and mass eigenstates are given by

$$\begin{pmatrix} \psi_\nu \\ \chi_\ell \end{pmatrix} = U_\alpha \begin{pmatrix} N_1 \\ N_2 \end{pmatrix}. \tag{3}$$

The following relations can be obtained from the above equations:

$$\begin{aligned}
M_{\psi_\ell} &= M_{N_1} \cos^2 \alpha + M_{N_2} \sin^2 \alpha, \\
M_{\chi_\ell} &= M_{N_1} \sin^2 \alpha + M_{N_2} \cos^2 \alpha, \\
M_D &= \Delta M \sin \alpha \cos \alpha, \tag{4}
\end{aligned}$$

with  $\Delta M = (M_{N_1} - M_{N_2})$  representing the mass splitting between neutral mass eigenstates. The lightest neutral eigenstate ( $N_2$ ) is the DM candidate in the present model. Its annihilations and co-annihilations with other neutral eigenstate ( $N_1$ ) and charged lepton ( $\psi_l$ )

provide relic abundance of the Universe. The mass of charged lepton is  $M_{\psi_\ell}$  and the mass of both components of  $\psi_q$  are equal to  $M_{\psi_q}$ . In the whole analysis, we consider mass of leptoquark  $M_{S_1} = 1.2$  TeV.

### III. DARK SECTOR

#### A. Relic abundance

To compute the freeze-out abundance of vector-like leptonic DM, we utilize the well-known packages, LanHEP [91] for model implementation and micrOMEGAs [92–94] for DM study. The relic density is mainly dictated by three parameters i.e., the mass splitting  $\Delta M$ ,  $y_\ell$  and  $y'_\ell$ . The mass splitting controls the co-annihilation contribution and the Yukawa determines the impact of LQ portal channels on relic density.

All the possible annihilation and co-annihilation channels are displayed in Figs. 1 and 2. For lower mass splitting, co-annihilation channels of charged and neutral vector-like components (i.e.,  $N_2, N_1, \psi_l$ ) can contribute to the total cross section, the impact is made clear in left panel of Fig. 3. The effect of LQ portal channels is directed by the Yukawa  $y_\ell$ , illustrated in the right panel of Fig. 3.

#### B. Direct detection

In the present model, the DM can scatter off nucleus in the detector, leaving a footprint through the following effective interactions

$$\begin{aligned} \mathcal{L}_Z^{\text{eff}} &\sim b_q(\bar{q}\gamma^\mu q)(\overline{N_2}\gamma_\mu N_2), \quad b_q = \frac{\sin^2 \alpha}{2M_Z^2}(g' \sin \theta_w + g \cos \theta_w) \frac{gC_V^q}{2 \cos \theta_w}, \\ \mathcal{L}_h^{\text{eff}} &\sim a_q(\bar{q}q)(\overline{N_2}N_2), \quad a_q = \frac{\sqrt{2}M_q y_D \sin \alpha \cos \alpha}{M_h^2 v}, \\ \mathcal{L}_{S_1}^{\text{eff}} &\sim c_q(\bar{q}\gamma^\mu q)(\overline{N_2}\gamma_\mu N_2) + c'_q(\bar{q}\gamma^\mu \gamma^5 q)(\overline{N_2}\gamma_\mu \gamma^5 N_2), \quad c_q = c'_q = \frac{y_\ell^2 \sin^2 \alpha - y_\ell'^2 \cos^2 \alpha}{8M_{S_1}^2}. \end{aligned} \quad (5)$$

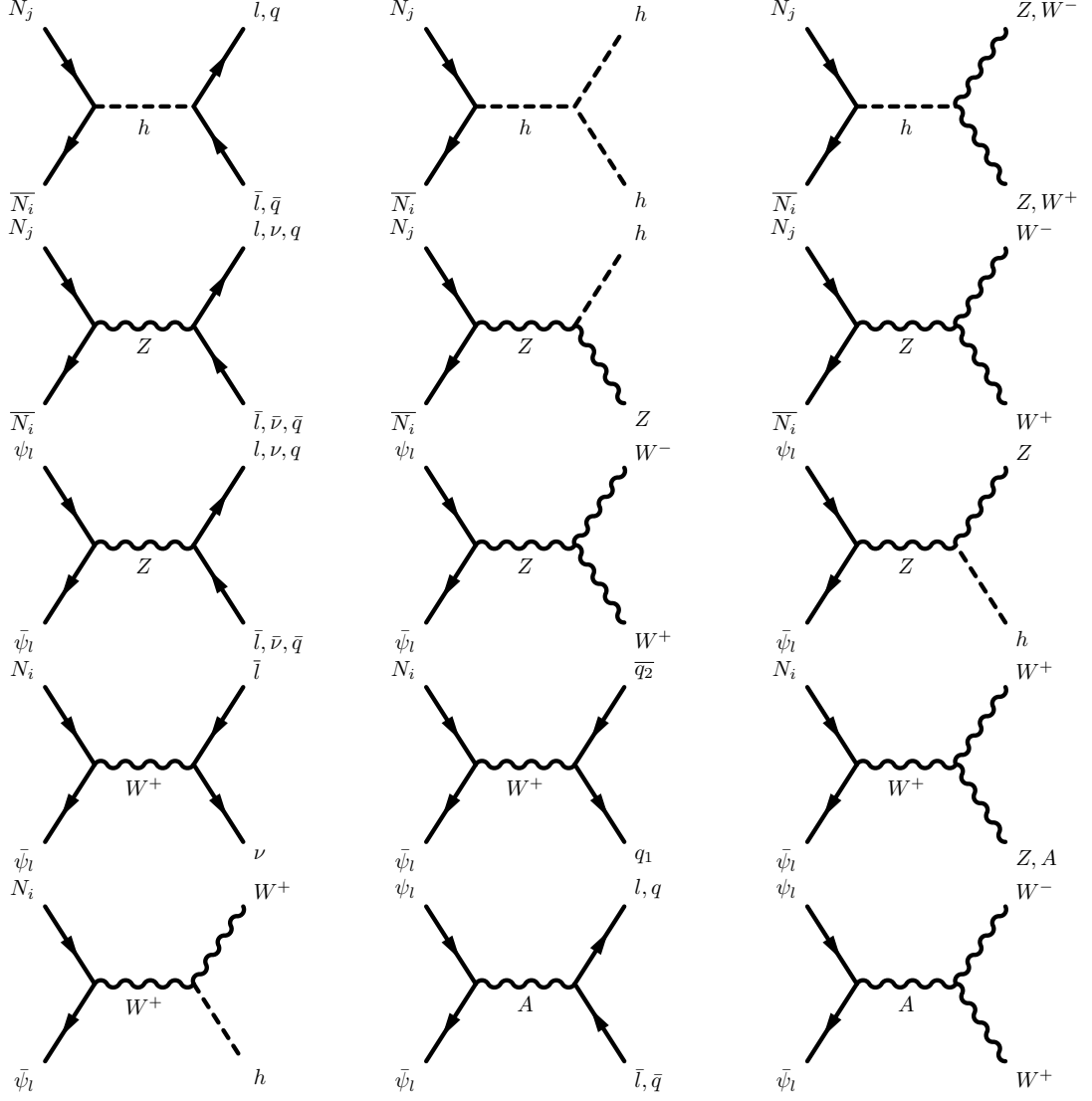


FIG. 1: Annihilation and co-annihilation channels mediated by SM bosons.

The interaction is represented as Feynman diagrams in Fig. 4 and the corresponding WIMP-nucleon cross sections are given by

$$\begin{aligned}
\sigma_Z^{\text{SI}} &= \frac{\mu^2}{\pi} [Zb_p + (A - Z)b_n]^2, \quad b_p = 2b_u + b_d, b_n = b_u + 2b_d, \\
\sigma_h^{\text{SI}} &= \frac{\mu^2}{\pi} [Zf_p + (A - Z)f_n]^2, \quad f_{p(n)} = \frac{a_q}{M_q} \left[ \frac{2}{9} + \frac{7}{9} (f_{Tu}^{p(n)} + f_{Td}^{p(n)} + f_{Ts}^{p(n)}) \right], \\
\sigma_{S_1}^{\text{SI}} &= \frac{\mu^2}{\pi} [Zc_p + (A - Z)c_n]^2, \quad c_p = c_d, c_n = 2c_d, \\
\sigma_{S_1}^{\text{SD}} &= \frac{4\mu^2}{\pi} [c'_d \Delta_d + c'_s \Delta_s]^2 J_N (J_N + 1).
\end{aligned} \tag{6}$$

Here  $J_N = 1/2$ , the typical values of  $f_{Tq}^{p(n)}$  and quark spin functions  $\Delta_q$  are provided in [95].

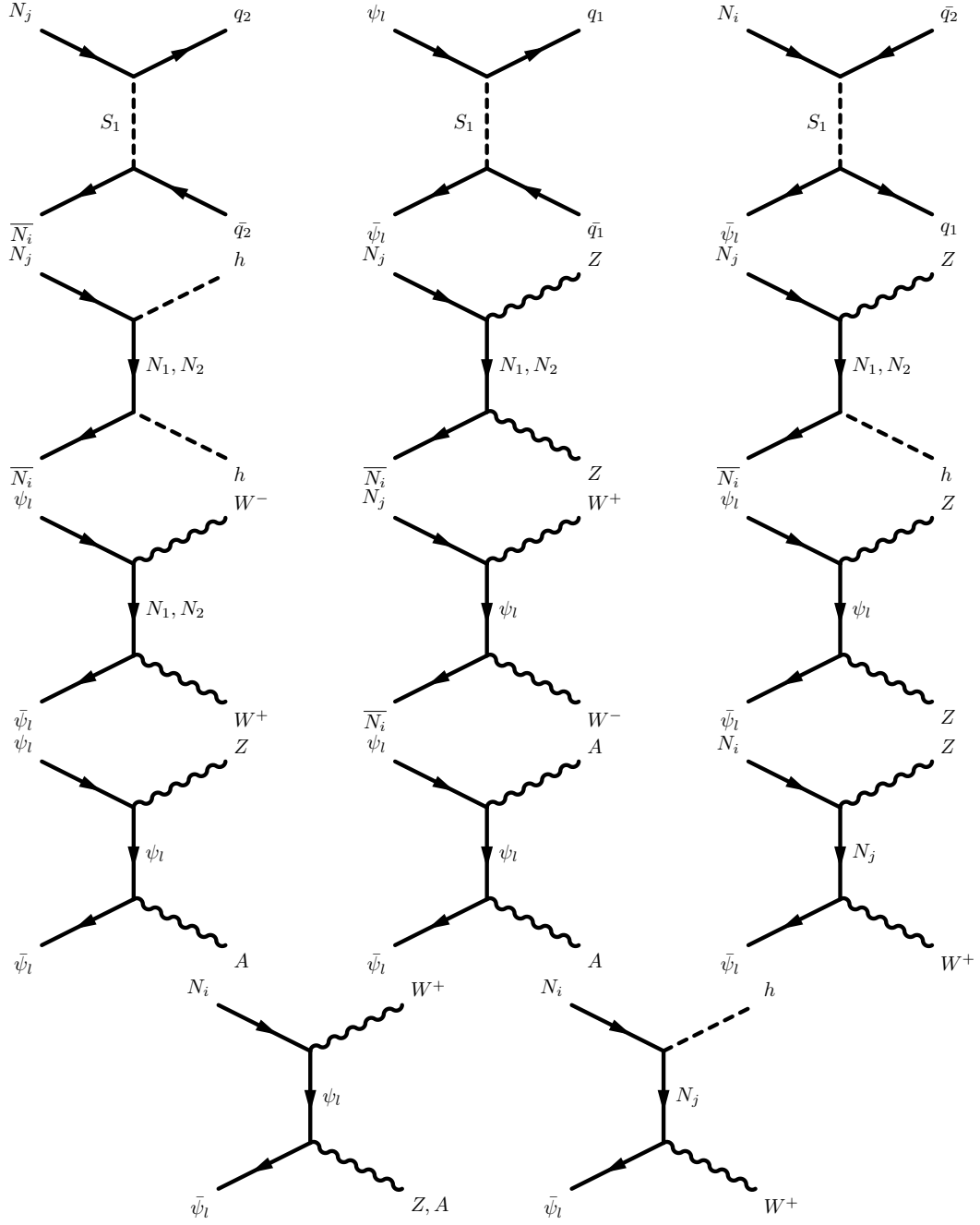


FIG. 2: Annihilation and co-annihilation channels via new fields portal, where  $q_1 = u, c, t$  and  $q_2 = d, s, b$ .

The smallness of singlet-doublet mixing plays a crucial role in getting the  $Z$ -portal spin-independent (SI) cross-section within experimental bound of XENON1T [96]. In other words, an upper limit on mixing parameter  $\alpha$  ( $\sim 10^{-3}$ ) is levied, as shown in the left plot (upper panel) of Fig. 5. The same logic is applicable in the context of SLQ portal vectorial

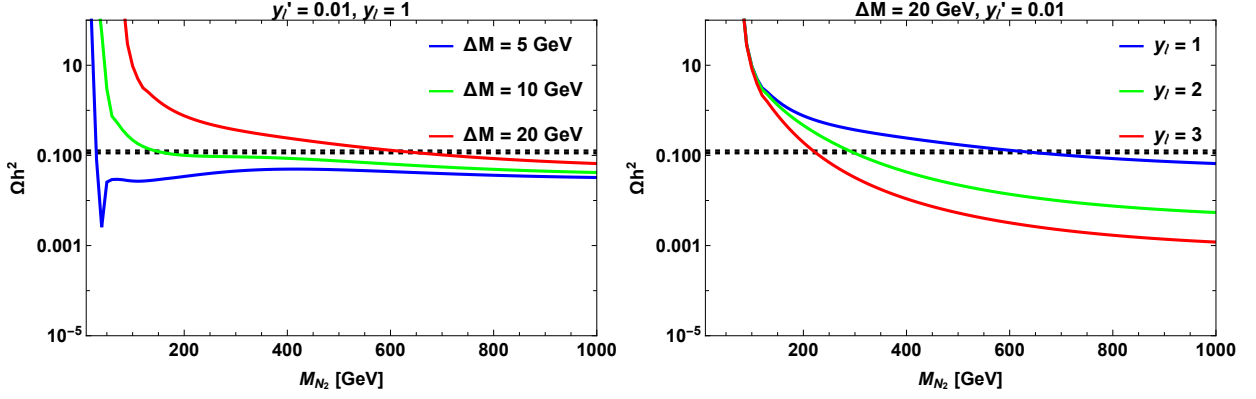


FIG. 3: Relic density as a function of DM mass. Horizontal dashed lines correspond to Planck limit [72] in  $3\sigma$  region.

part, allowing large Yukawa  $y_\ell$  with SI contribution still consistent with XENON1T limit, as displayed in the left plot (lower panel) of Fig. 5. Right plot in the upper panel corresponds to Higgs-mediated SI contribution, which depends on the mass splitting  $\Delta M$ . Lower right panel projects SD contribution of axial vector part in SLQ-portal. Above figures suggest the model is safe from the stringent upper limits of XENON1T [96] and PICO-60 [97].

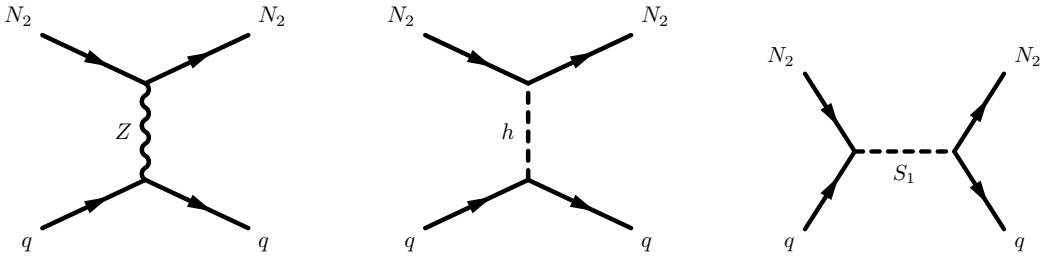


FIG. 4: Feynman diagrams for direct detection.



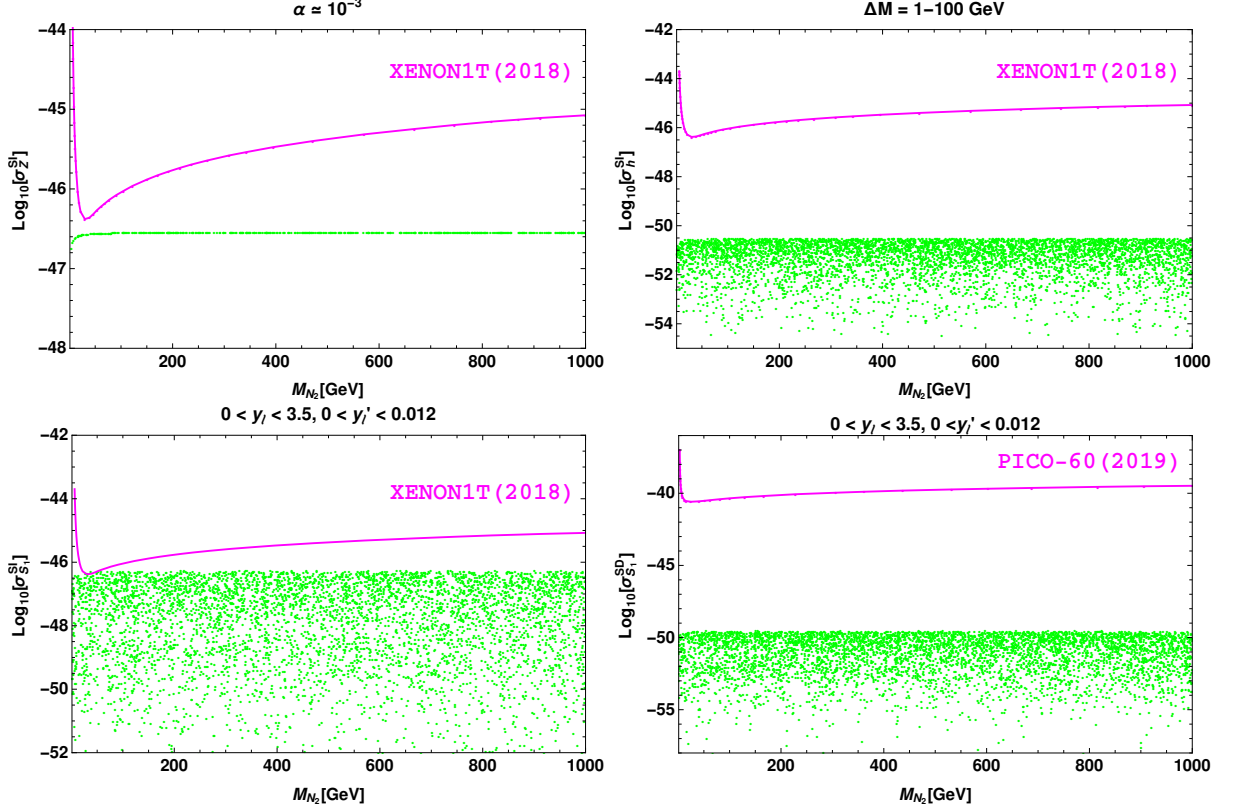


FIG. 5: WIMP-nucleon cross section in various portals. Magenta lines correspond to upper limits from XENON1T [96] and PICO-60 [97].

#### IV. ELECTROWEAK PRECISION PARAMETERS

The vector-like fermions in the present model can alter the vacuum polarization of SM gauge bosons. The relevant interaction Lagrangian terms read as

$$\begin{aligned}
\mathcal{L}_\ell \supset & \left( \frac{g}{2} W_\mu^3 - \frac{g'}{2} B_\mu \right) (\bar{\psi}_\nu \gamma^\mu \psi_\nu) + \frac{g}{\sqrt{2}} W_\mu^+ (\bar{\psi}_\nu \gamma^\mu \psi_l) + \frac{g}{\sqrt{2}} W_\mu^- (\bar{\psi}_l \gamma^\mu \psi_\nu) \\
& - \left( \frac{g}{2} W_\mu^3 + \frac{g'}{2} B_\mu \right) (\bar{\psi}_l \gamma^\mu \psi_l), \tag{7}
\end{aligned}$$

$$\begin{aligned}
\mathcal{L}_q \supset & \left( \frac{g}{2} W_\mu^3 + \frac{g'}{6} B_\mu \right) (\bar{\psi}_u \gamma^\mu \psi_u) + \frac{g}{\sqrt{2}} W_\mu^+ (\bar{\psi}_u \gamma^\mu \psi_d) + \frac{g}{\sqrt{2}} W_\mu^- (\bar{\psi}_d \gamma^\mu \psi_u) \\
& - \left( \frac{g}{2} W_\mu^3 - \frac{g'}{6} B_\mu \right) (\bar{\psi}_d \gamma^\mu \psi_d). \tag{8}
\end{aligned}$$

For the above gauge interactions, the electroweak precision (EWP) parameters are given by [98]

$$\begin{aligned}
\hat{S} &= \frac{g}{g'} \times \Pi'_{W_3 B}(0), \\
\hat{T} &= \frac{1}{M_W^2} (\Pi_{W_3 W_3}(0) - \Pi_{W^+ W^-}(0)), \\
Y &= \frac{M_W^2}{2} \times \Pi''_{BB}(0), \\
W &= \frac{M_W^2}{2} \times \Pi''_{W_3 W_3}(0).
\end{aligned} \tag{9}$$

The details of  $\Pi$  functions are provided in Appendix A. In the context of vector-like leptons, the mass splitting of neutral components ( $\Delta M$ ) dictate the above parameters. In Fig. 6, we display the region of parameters which are DM consistent i.e., Planck  $3\sigma$  bound on relic density and also limits on WIMP-nucleon cross section from XENON1T and PICO-60. Using the limits of global fit on the precision parameters [99], the favorable region in the context of precision measurements is also presented.  $Y$  and  $W$  parameters seem to disfavor low mass splittings. No relevant constraint on the masses of vector-like quarks is obtained from electroweak precision parameters.

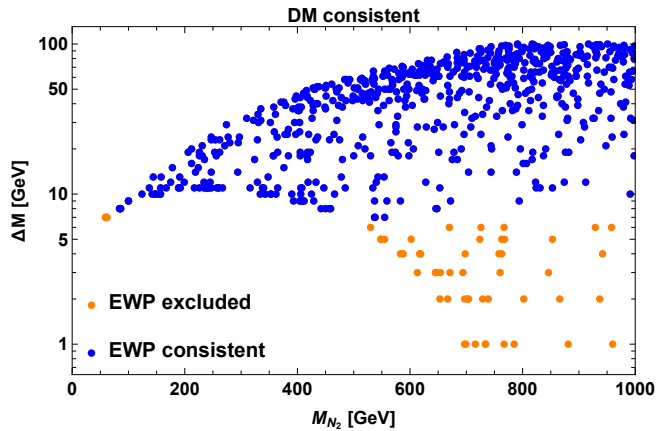


FIG. 6: Model parameter space with DM and EWP constraints.

## V. CONSTRAINTS FROM THE QUARK SECTOR

In this section, we explain the flavor anomalies through one loop box diagrams. The rare FCNC  $b \rightarrow s$  transitions can proceed by the generic box diagrams in the presence of

an additional scalar LQ and the vector-like fermion doublets. The relevant new parameters governing these transitions are the Yukawa-like couplings  $(y_\ell^{(\prime)}, y_q)$  and the masses of new particles  $(M_{\psi_q}, M_{\psi_l}, M_{N_1}, M_{N_2})$ . The available new parameter space consistent with the experimental limits of the DM observables are discussed in the previous section. Nevertheless, the quark sector can further constrain these parameters, which will be presented in the subsequent sections.

### A. $b \rightarrow sll$

The effective Hamiltonian describing the  $b \rightarrow sl^+l^-$  quark level transition is given by [100, 101]

$$\mathcal{H}_{\text{eff}} = -\frac{4G_F}{\sqrt{2}}\lambda_t \left[ \sum_{i=1}^6 C_i(\mu)\mathcal{O}_i + \sum_{i=7,9,10} (C_i(\mu)\mathcal{O}_i + C'_i(\mu)\mathcal{O}'_i) \right], \quad (10)$$

where  $C_i$ 's are the Wilson coefficients [102] and  $\mathcal{O}_i$ 's are the corresponding four-fermion operators, given as

$$\begin{aligned} O_7^{(\prime)} &= \frac{e}{16\pi^2} \left( \bar{s}\sigma_{\mu\nu} (m_s P_{L(R)} + m_b P_{R(L)}) b \right) F^{\mu\nu}, \\ O_9^{(\prime)} &= \frac{\alpha_{\text{em}}}{4\pi} (\bar{s}\gamma^\mu P_{L(R)} b) (\bar{l}\gamma_\mu l), \quad O_{10}^{(\prime)} = \frac{\alpha_{\text{em}}}{4\pi} (\bar{s}\gamma^\mu P_{L(R)} b) (\bar{l}\gamma_\mu \gamma_5 l), \end{aligned} \quad (11)$$

with  $\alpha_{\text{em}}$  as the fine-structure constant and  $P_{L,R} = (1 \mp \gamma_5)/2$  are the chiral operators. In the SM, though the primed Wilson coefficients ( $C'_i$ ) are zero, but they can have non-vanishing values in the NP models beyond the SM. In the presence of scalar LQ, the one loop box diagram responsible for the rare decay processes involving  $b \rightarrow sll$  quark level transition is depicted in Fig. 7.

Due to the exchange of leptoquark and new vector like fermions, we obtain additional contribution to the SM amplitude and the new Wilson coefficients are given as

$$\begin{aligned} C_9^{\text{NP}} = -C_{10}^{\text{NP}} &= -\frac{\sqrt{2}|y_q|^2}{512\pi G_F \alpha_{\text{em}} \lambda_t M_{S_1}^2} \times \left[ |y_\ell \cos \alpha - y'_\ell \sin \alpha|^2 F(x_u, x_{N_1}) \right. \\ &\quad \left. + |y_\ell \sin \alpha + y'_\ell \cos \alpha|^2 F(x_u, x_{N_2}) + |y'_q|^2 F(x_u, x_u) \right], \end{aligned} \quad (12)$$

where  $x_{N_1} = M_{N_1}^2 \cos^2 \alpha / M_{S_1}^2$ ,  $x_{N_2} = M_{N_2}^2 \sin^2 \alpha / M_{S_1}^2$ ,  $x_u = M_{\psi_u}^2 / M_{S_1}^2$  and the loop function has the form

$$F(x_i, x_j) = \frac{1}{(1-x_i)(1-x_j)} + \frac{x_i^2 \log x_i}{(1-x_i)^2(x_i-x_j)} + \frac{x_j^2 \log x_j}{(1-x_j)^2(x_j-x_i)}. \quad (13)$$

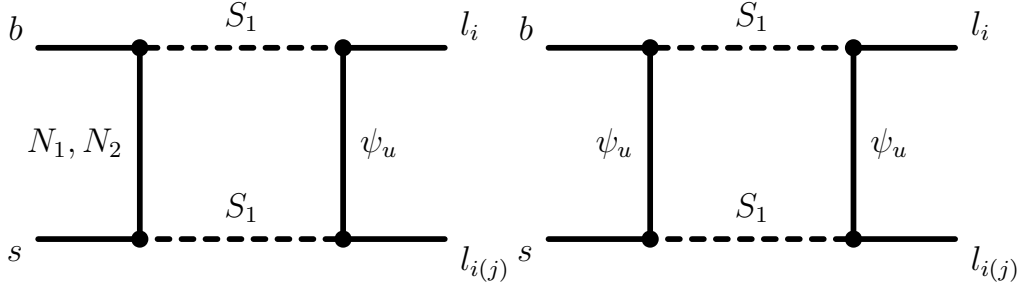


FIG. 7: One-loop box diagrams of  $b \rightarrow sl_i l_{i(j)}$  processes with scalar leptoquark and vector-like fermions in the loop.

We assume that the NP contribution to  $b \rightarrow see$  transition is negligible i.e., we consider  $b \rightarrow see$  transition is SM like.

### $B_s \rightarrow l^+ l^-$

In the presence of new Wilson coefficient, the branching ratio of  $B_s \rightarrow l^+ l^-$  process is given by

$$\text{Br}(B_s \rightarrow l^+ l^-) = \frac{G_F^2}{16\pi^3} \tau_{B_s} \alpha^2 f_{B_s}^2 M_{B_s} m_l^2 |V_{tb} V_{ts}^*|^2 \sqrt{1 - \frac{4m_l^2}{M_{B_s}^2}} |C_{10}^{\text{SM}} + C_{10}^{\text{NP}}|^2. \quad (14)$$

The experimental limits on branching ratios of  $B_s \rightarrow \mu^+ \mu^- (\tau^+ \tau^-)$  processes and the corresponding predicted SM values by using the relevant input parameters from [103] are given by

$$\begin{aligned} \text{Br}(B_s \rightarrow \mu\mu)^{\text{SM}} &= (3.65 \pm 0.23) \times 10^{-9}, & \text{Br}(B_s \rightarrow \mu\mu)^{\text{Expt}} &= (2.7_{-0.5}^{+0.6}) \times 10^{-9}, \\ \text{Br}(B_s \rightarrow \tau\tau)^{\text{SM}} &= (7.73 \pm 0.49) \times 10^{-7}, & \text{Br}(B_s \rightarrow \tau\tau)^{\text{Expt}} &< 6.8 \times 10^{-3}. \end{aligned} \quad (15)$$

### $B \rightarrow Kll$

The differential branching ratio of  $B \rightarrow Kll$  process with respect to  $q^2$  is given by [18]

$$\frac{d\text{Br}(B \rightarrow Kll)}{dq^2} = \tau_B \frac{G_F^2 \alpha_{\text{em}}^2 |V_{tb} V_{ts}^*|^2}{2^8 \pi^5 M_B^3} \sqrt{\lambda(M_B^2, M_K^2, q^2)} \beta_l f_+^2 \left( a_l(q^2) + \frac{c_l(q^2)}{3} \right), \quad (16)$$

where

$$\begin{aligned}
a_l(q^2) &= q^2 |F_P|^2 + \frac{\lambda(M_B^2, M_K^2, q^2)}{4} (|F_A|^2 + |F_V|^2) \\
&\quad + 2m_l(M_B^2 - M_K^2 + q^2) \text{Re}(F_P F_A^*) + 4m_l^2 M_B^2 |F_A|^2, \\
c_l(q^2) &= -\frac{\lambda(M_B^2, M_K^2, q^2)}{4} \beta_l^2 (|F_A|^2 + |F_V|^2),
\end{aligned} \tag{17}$$

with

$$\begin{aligned}
F_V &= \frac{2m_b}{M_B} C_7^{\text{eff}} + C_9^{\text{eff}} + C_9^{\text{NP}}, \quad F_A = C_{10}^{\text{SM}} + C_{10}^{\text{NP}}, \\
F_P &= m_l (C_{10}^{\text{SM}} + C_{10}^{\text{NP}}) \left[ \frac{M_B^2 - M_K^2}{q^2} \left( \frac{f_0(q^2)}{f_+(q^2)} - 1 \right) - 1 \right],
\end{aligned} \tag{18}$$

and

$$\lambda(a, b, c) = a^2 + b^2 + c^2 - 2(ab + bc + ca), \quad \beta_l = \sqrt{1 - 4m_l^2/q^2}. \tag{19}$$

By using the input parameters from [103, 104], the predicted branching ratios of  $B \rightarrow K\mu\mu(\tau\tau)$  processes and the corresponding experimental data [103] are given by

$$\begin{aligned}
\text{Br}(B^0 \rightarrow K^0 \mu^+ \mu^-)^{\text{SM}} &= (1.48 \pm 0.12) \times 10^{-7}, \quad \text{Br}(B^0 \rightarrow K^0 \mu^+ \mu^-)^{\text{Expt}} = (3.39 \pm 0.34) \times 10^{-7}, \\
\text{Br}(B^+ \rightarrow K^+ \mu^+ \mu^-)^{\text{SM}} &= (1.6 \pm 0.13) \times 10^{-7}, \quad \text{Br}(B^+ \rightarrow K^+ \mu^+ \mu^-)^{\text{Expt}} = (4.41 \pm 0.22) \times 10^{-7}, \\
\text{Br}(B^+ \rightarrow K^+ \tau^+ \tau^-)^{\text{SM}} &= (1.52 \pm 0.121) \times 10^{-7}, \quad \text{Br}(B^+ \rightarrow K^+ \tau^+ \tau^-)^{\text{Expt}} < 2.25 \times 10^{-3}.
\end{aligned} \tag{20}$$

### $B \rightarrow K^* l^+ l^-$

The differential decay rate of  $B \rightarrow K^* l^+ l^-$  process with respect to  $q^2$ , after integration over all angles;  $\theta_l$  (angle between  $l^-$  and  $B$  in the dilepton frame),  $\theta_{K^*}$  (angle between  $K^-$  and  $B$  in the  $K^- \pi^+$  frame) and  $\phi$  (angle between the normal of the  $K^- \pi^+$  and the dilepton planes) [105] is given by

$$\frac{d\Gamma}{dq^2} = \frac{3}{4} \left( J_1 - \frac{J_2}{3} \right), \quad J_{1,2} = 2J_{1,2}^s + J_{1,2}^c, \tag{21}$$

where the  $J_{1,2}^{s(c)}$  function in terms of transversity amplitudes are given in the Appendix B. The transversity amplitudes as a function of new Wilson coefficients are given as [106]

$$\begin{aligned}
A_{\perp L,R} &= N\sqrt{2\lambda(M_{K^*}^2, M_B^2, q^2)} \left[ ((C_9^{\text{eff}} + C_9^{\text{NP}}) \mp (C_{10}^{\text{SM}} + C_{10}^{\text{NP}})) \frac{V(q^2)}{M_B + M_{K^*}} + \frac{2m_b}{q^2} C_7 T_1(q^2) \right], \\
A_{\parallel L,R} &= -N\sqrt{2}(M_B^2 - M_{K^*}^2) \left[ ((C_9^{\text{eff}} + C_9^{\text{NP}}) \mp (C_{10}^{\text{SM}} + C_{10}^{\text{NP}})) \frac{A_1(q^2)}{M_B - M_{K^*}} + \frac{2m_b}{q^2} C_7 T_2(q^2) \right], \\
A_{0L,R} &= -\frac{N}{2M_{K^*}\sqrt{s}} \left[ ((C_9^{\text{eff}} + C_9^{\text{NP}}) \mp (C_{10}^{\text{SM}} + C_{10}^{\text{NP}})) \right. \\
&\quad \left. \times \left( (M_B^2 - M_{K^*}^2 - q^2)(M_B + M_{K^*})A_1(q^2) - \lambda(M_{K^*}^2, M_B^2, q^2) \frac{A_2(q^2)}{M_B + M_{K^*}} \right) \right], \\
A_t &= 2N\sqrt{\frac{\lambda(M_{K^*}^2, M_B^2, q^2)}{q^2}} (C_{10}^{\text{SM}} + C_{10}^{\text{NP}}) A_0(q^2), \tag{22}
\end{aligned}$$

where

$$N = V_{tb}V_{ts}^* \left[ \frac{G_F^2 \alpha_{\text{em}}^2}{3 \cdot 2^{10} \pi^5 M_B^3} q^2 \beta_l \sqrt{\lambda(M_{K^*}^2, M_B^2, q^2)} \right]^{1/2}. \tag{23}$$

With the use of the particle masses, life time of  $B$  meson and the  $B \rightarrow K^*$  form factor from [103, 107] the predicted  $B \rightarrow K^* l l$  branching ratios and the corresponding experimental data [103] are given by

$$\begin{aligned}
\text{Br}(B^0 \rightarrow K^{*0} \mu^+ \mu^-)^{\text{SM}} &= (1.967 \pm 0.158) \times 10^{-8}, \quad \text{Br}(B^0 \rightarrow K^{*0} \mu^+ \mu^-)^{\text{Expt}} = (9.4 \pm 0.5) \times 10^{-7}, \\
\text{Br}(B^+ \rightarrow K^{*+} \mu^+ \mu^-)^{\text{SM}} &= (1.758 \pm 0.141) \times 10^{-8}, \quad \text{Br}(B^+ \rightarrow K^{*+} \mu^+ \mu^-)^{\text{Expt}} < 5.9 \times 10^{-7}. \tag{24}
\end{aligned}$$

### $R_{K^{(*)}}$

The updated (full Run-I and Run-II LHCb data) value of the  $R_K$  lepton non-universality (LNU) parameter in the  $q^2 \in [1.1, 6]$  GeV<sup>2</sup> region [17]

$$R_K^{\text{LHCb21}} = \frac{\text{Br}(B^+ \rightarrow K^+ \mu^+ \mu^-)}{\text{Br}(B^+ \rightarrow K^+ e^+ e^-)} = 0.846_{-0.039-0.012}^{+0.042+0.013}, \tag{25}$$

provides the disagreement of  $3.1\sigma$  from the SM prediction [18, 19]

$$R_K^{\text{SM}} = 1.0003 \pm 0.0001. \tag{26}$$

Analogous measurements by the LHCb Collaboration on  $R_{K^*}$  ratio in two low- $q^2$  bins [3]

$$R_{K^*}^{\text{LHCb}} = \begin{cases} 0.660_{-0.070}^{+0.110} \pm 0.03 & q^2 \in [0.045, 1.1] \text{ GeV}^2, \\ 0.69_{-0.07}^{+0.11} \pm 0.05 & q^2 \in [1.1, 6.0] \text{ GeV}^2, \end{cases} \tag{27}$$

have  $2.1\sigma$  and  $2.5\sigma$  deviations from their corresponding SM values respectively [20]

$$R_{K^*}^{\text{SM}} = \begin{cases} 0.92 \pm 0.02 & q^2 \in [0.045, 1.1] \text{ GeV}^2, \\ 1.00 \pm 0.01 & q^2 \in [1.1, 6.0] \text{ GeV}^2. \end{cases} \quad (28)$$

Though the Belle experiment [4, 108] has measured the  $R_{K^{(*)}}$  parameters but their results have comparatively larger uncertainties.

### B. $b \rightarrow s\nu_l\bar{\nu}_l$

The effective Hamiltonian of lepton flavor conserving  $b \rightarrow s\nu_i\bar{\nu}_i$  process is given by [109, 110]

$$\mathcal{H}_{\text{eff}}^{\nu\nu} = -\frac{4G_F}{\sqrt{2}}\lambda_t C_L^{\text{SM}}\mathcal{O}_L, \quad (29)$$

where

$$\mathcal{O}_L = \frac{\alpha_{\text{em}}}{4\pi}[\bar{s}\gamma^\mu P_L b][\bar{\nu}_i\gamma_\mu(1-\gamma^5)\nu_i], \quad (30)$$

is the six dimensional operator,  $C_L^{\text{SM}} \approx -X(x_t)/\sin^2\theta_W$  is the SM Wilson coefficient calculated using the loop function  $X(x_t)$  [111] and  $\theta_W$  is the weak mixing angle. Here  $C_L^{ij}$  is zero in the SM. Fig. 8 depicts the  $b \rightarrow s\nu_l\bar{\nu}_l$  decay mode in the presence of SLQ and vector-like

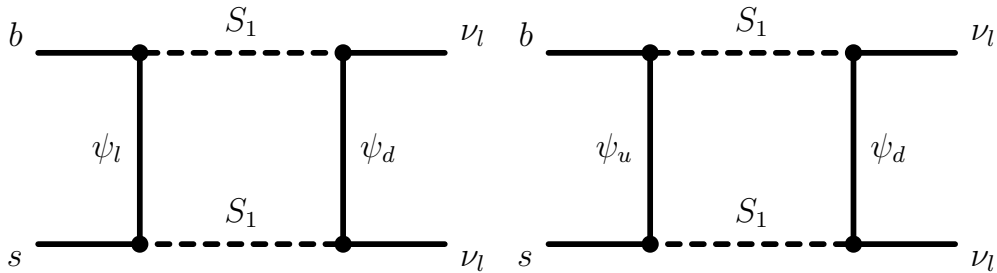


FIG. 8: One-loop box diagrams of  $b \rightarrow s\nu_l\bar{\nu}_l$  processes with scalar leptoquark and vector-like fermions in the loop.

quarks/leptons. The additional NP contribution to the SM Wilson coefficient is given by

$$C_L^{\text{NP}} = -\frac{\sqrt{2}|y_q|^2}{512\pi G_F\alpha_{\text{em}}\lambda_t M_{S_1}^2} \left[ |y_\ell|^2 F(x_d, x_l) + |y'_q|^2 F(x_d, x_u) \right], \quad (31)$$

where  $x_i = M_i^2/M_{S_1}^2$  with  $i = \psi_d, \psi_u, \psi_l$ .

### $B \rightarrow K \nu_l \bar{\nu}_l$

The branching ratio of  $B \rightarrow K \nu_l \bar{\nu}_l$  decay process in the presence of new Wilson coefficient is given by [112]

$$\frac{d\text{Br}}{ds_B} = \tau_B \frac{G_F^2 \alpha^2}{256 \pi^5} |V_{ts}^* V_{tb}|^2 M_B^5 \lambda^{3/2}(s_B, \tilde{M}_K^2, 1) |f_+^K(s_B)|^2 |C_L^{\text{SM}} + C_L^{\text{NP}}|^2, \quad (32)$$

where  $\tilde{M}_i = M_i/M_B$ ,  $s_B = s/M_B^2$ . Since the different neutrino flavors in the decays  $b \rightarrow s \nu_l \bar{\nu}_l$  are not distinguished experimentally, the decay rate will be multiplied with an extra factor 3. By using input values from [103], the predicted branching ratio values of  $B^{+(0)} \rightarrow K^{+(0)} \nu_l \bar{\nu}_l$  and the corresponding experimental limits are given by

$$\begin{aligned} \text{Br}(B^0 \rightarrow K^0 \nu_l \bar{\nu}_l)^{\text{SM}} &= (4.53 \pm 0.267) \times 10^{-6}, \quad \text{Br}(B^0 \rightarrow K^0 \nu_l \bar{\nu}_l)^{\text{Expt}} < 2.6 \times 10^{-5}, \\ \text{Br}(B^+ \rightarrow K^+ \nu_l \bar{\nu}_l)^{\text{SM}} &= (4.9 \pm 0.288) \times 10^{-6}, \quad \text{Br}(B^+ \rightarrow K^+ \nu_l \bar{\nu}_l)^{\text{Expt}} < 1.6 \times 10^{-5}. \end{aligned} \quad (33)$$

### $B_{(s)} \rightarrow K^*(\phi) \nu_l \bar{\nu}_l$

In the presence of new physics, the decay rate of  $B \rightarrow K^* \nu \bar{\nu}$  process with respect to the  $s_B$  and  $\cos \theta$  is given as [112, 113]

$$\frac{d^2\Gamma}{ds_B d\cos\theta} = \frac{3}{4} \frac{d\Gamma_T}{ds_B} \sin^2 \theta + \frac{3}{2} \frac{d\Gamma_L}{ds_B} \cos^2 \theta, \quad (34)$$

where the longitudinal and transverse polarization decay rates are

$$\frac{d\Gamma_L}{ds_B} = 3m_B^2 |A_0|^2, \quad \frac{d\Gamma_T}{ds_B} = 3m_B^2 (|A_\perp|^2 + |A_\parallel|^2), \quad (35)$$

with the transversity amplitudes,  $A_{0,\perp,\parallel}$  in terms of form factor and new Wilson coefficients are defined as

$$\begin{aligned} A_0(s_B) &= -\frac{N(C_L^{\text{SM}} + C_L^{\text{NP}})}{\tilde{M}_{K^*} \sqrt{s_B}} \left[ (1 - \tilde{M}_{K^*}^2 - s_B)(1 + \tilde{M}_{K^*}) A_1(s_B) - \lambda(1, \tilde{M}_{K^*}^2, s_B) \frac{A_2(s_B)}{1 + \tilde{M}_{K^*}} \right], \\ A_\perp(s_B) &= 2N \sqrt{2} \lambda^{1/2}(1, \tilde{M}_{K^*}^2, s_B) (C_L^{\text{SM}} + C_L^{\text{NP}}) \frac{V(s_B)}{(1 + \tilde{M}_{K^*})}, \\ A_\parallel(s_B) &= -2N \sqrt{2} (1 + \tilde{M}_{K^*}) (C_L^{\text{SM}} + C_L^{\text{NP}}) A_1(s_B), \end{aligned} \quad (36)$$

where

$$N = V_{tb} V_{ts}^* \left[ \frac{G_F^2 \alpha^2 M_B^3}{3 \cdot 2^{10} \pi^5} s_B \lambda^{1/2}(1, \tilde{M}_{K^*}^2, s_B) \right]^{1/2}. \quad (37)$$



Using all the required input values from [103, 107], the branching ratio of  $B_{(s)} \rightarrow K^*(\phi)\nu\bar{\nu}$  and their corresponding experimental limits [103] are given by

$$\begin{aligned} \text{Br}(B^0 \rightarrow K^{*0}\nu_l\bar{\nu}_l)^{\text{SM}} &= (9.48 \pm 0.752) \times 10^{-6}, \quad \text{Br}(B^0 \rightarrow K^{*0}\nu_l\bar{\nu}_l)^{\text{Expt}} < 1.8 \times 10^{-5}, \\ \text{Br}(B^+ \rightarrow K^{*+}\nu_l\bar{\nu}_l)^{\text{SM}} &= (1.03 \pm 0.06) \times 10^{-5}, \quad \text{Br}(B^+ \rightarrow K^{*+}\nu_l\bar{\nu}_l)^{\text{Expt}} < 4.0 \times 10^{-5}, \\ \text{Br}(B_s \rightarrow \phi\nu_l\bar{\nu}_l)^{\text{SM}} &= (1.2 \pm 0.07) \times 10^{-5}, \quad \text{Br}(B_s \rightarrow \phi\nu_l\bar{\nu}_l)^{\text{Expt}} < 5.4 \times 10^{-3}. \end{aligned} \quad (38)$$

### C. $b \rightarrow s\gamma$

In Fig. 9, we present the diagrams of one loop contributions to  $b \rightarrow s\gamma$  processes with scalar leptoquark and vector-like fermions as the internal lines in the loop. Including the

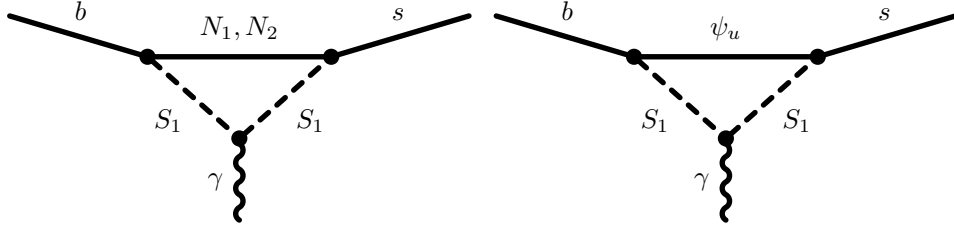


FIG. 9: One-loop diagrams of  $b \rightarrow s\gamma$  processes with scalar leptoquark and vector-like fermions in the loop.

NP contribution, the effective Hamiltonian of  $b \rightarrow s\gamma$  decay modes is given by

$$\mathcal{H}_{\text{eff}}^{\gamma} = -\frac{4G_F}{\sqrt{2}}V_{tb}V_{ts}^*(C_7^{\gamma\text{SM}} + C_7^{\gamma\text{NP}})\mathcal{O}_7, \quad (39)$$

where the new  $C_7^{\gamma\text{NP}}$  Wilson coefficient is given by

$$\begin{aligned} C_7^{\gamma\text{NP}} &= -\frac{\sqrt{2}}{24G_FV_{tb}V_{ts}^*M_{S_1}^2} \times \left[ |y_{\ell} \cos \alpha - y'_{\ell} \sin \alpha|^2 \tilde{F}_7(x_{N_1}) + |y_{\ell} \sin \alpha + y'_{\ell} \cos \alpha|^2 \tilde{F}_7(x_{N_2}) \right. \\ &\quad \left. + |y'_q|^2 \left( \tilde{F}_7(x_u) + 2F_7(x_u) \right) \right], \end{aligned} \quad (40)$$

with

$$F_7(x) = \frac{x^3 - 6x^2 + 6x \log x + 3x + 2}{12(x-1)^4}, \quad \tilde{F}_7(x) = x^{-1}F_7(x^{-1}). \quad (41)$$

## $\bar{B} \rightarrow X_s \gamma$

Including the SLQ and vector-like fermions contributions, the total branching ratio of  $B \rightarrow X_s \gamma$  decay mode is given by

$$\text{Br}(\bar{B} \rightarrow X_s \gamma) = \text{Br}(\bar{B} \rightarrow X_s \gamma)|^{\text{SM}} \left( 1 + \frac{C_7^{\gamma\text{NP}}}{C_7^{\gamma\text{SM}}} \right)^2. \quad (42)$$

The SM branching ratio values [114] and the corresponding experimental limit [115] of  $B \rightarrow X_s \gamma$  decay mode is given by

$$\begin{aligned} \text{Br}(\bar{B} \rightarrow X_s \gamma)_{E_\gamma > 1.6 \text{ GeV}}^{\text{SM}} &= (3.36 \pm 0.23) \times 10^{-4}, \\ \text{Br}(\bar{B} \rightarrow X_s \gamma)_{E_\gamma > 1.6 \text{ GeV}}^{\text{Expt}} &= (3.32 \pm 0.16) \times 10^{-4}. \end{aligned} \quad (43)$$

## D. Muon anomalous magnetic moment

The long sustaining discrepancy between the experimental measurements and SM value of muon anomalous magnetic moment took further step with the recent observations from Fermilab. Earlier, E821 experiment at Brookhaven National laboratory [116] has reported a deviation of  $3.3\sigma$  from SM prediction [117]

$$\Delta a_\mu^{\text{BNL}} = a_\mu^{\text{exp}} - a_\mu^{\text{SM}} = (26.1 \pm 7.9) \times 10^{-10}. \quad (44)$$

With lattice calculations, the deviation mounts to  $3.7\sigma$  [118, 119]. Recently, Fermilab's E989 experiment [120] has announced a discrepancy of  $4.2\sigma$

$$\Delta a_\mu^{\text{FNAL}} = (25.1 \pm 5.9) \times 10^{-10}. \quad (45)$$

The absolute magnitude of the discrepancy between the SM prediction and the experimental value is small and can be accommodate by adding the new physics contributions. Fig. 10 represents the one loop contribution to the muon anomalous magnetic moment with scalar leptoquark and vector-like quark in the loop.

The scalar LQ contribution to  $a_\mu$  is

$$\Delta a_\mu = \frac{m_\mu^2 (y_q)^2}{8\pi^2 M_{S_1}^2} \left( 2(f_1(x_u) + f_2(x_u)) - (\bar{f}_1(x_u) + \bar{f}_2(x_u)) \right), \quad (46)$$

where the functions  $f_{1,2}(x_u)$  and  $\bar{f}_{1,2}(x_u)$  are defined in Appendix C.

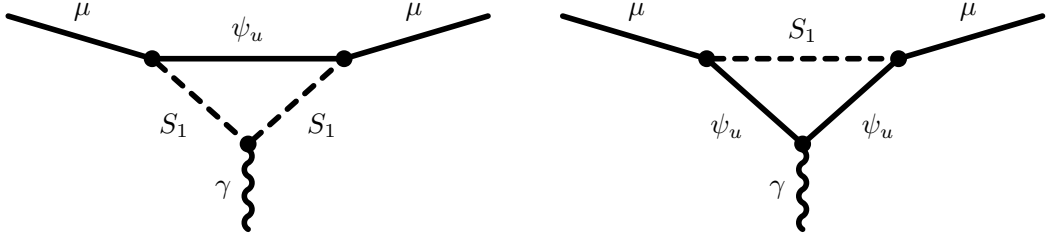


FIG. 10: One-loop contribution to muon anomalous magnetic moment with scalar leptoquark and vector-like fermion in the loop.

Using all the above discussed observables, the predicted allowed region for  $y'_q - y_q$  (left panel) and  $y'_\ell - y_\ell$  (right panel) parameters are presented in Fig. 11 and the allowed parameter space are given in Table II.

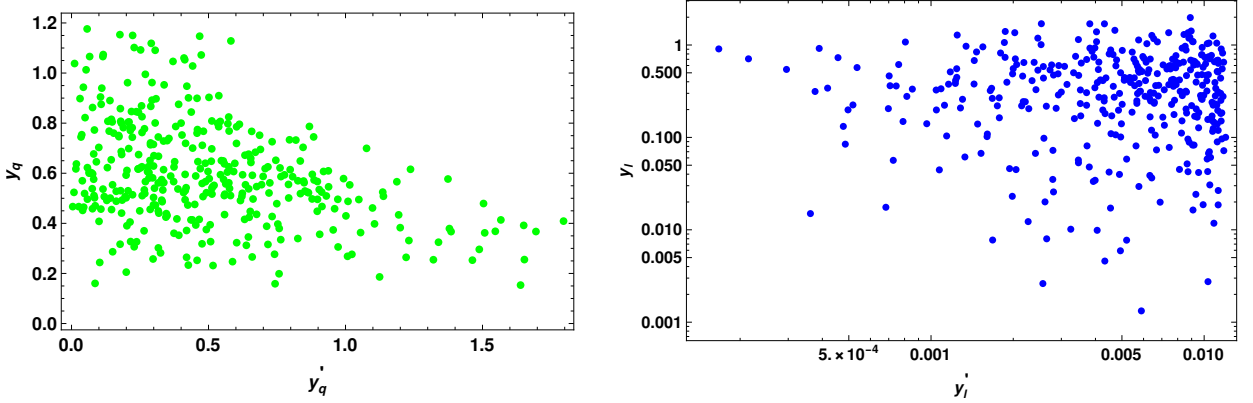


FIG. 11: Constraints on  $y'_q - y_q$  (left panel) and  $y'_\ell - y_\ell$  (right panel) parameters obtained from the branching ratios of  $B \rightarrow K^{(*)}l^+l^-(\nu_l\bar{\nu}_l)$ ,  $B_s \rightarrow ll$  ( $l = \mu, \tau$ ),  $\bar{B} \rightarrow X_s\gamma$  processes,  $R_{K^{(*)}}$  ratios and the muon anomalous magnetic moment.

Parameters	$y_q$	$y'_q$	$y_\ell$	$y'_\ell$
Allowed values	0 – 1.2	0 – 1.8	0 – 2.0	0 – 0.012

TABLE II: Allowed parameter space of  $y_q^{(l)}$  and  $y_\ell^{(l)}$ .

## VI. IMPACT ON LEPTON FLAVOR VIOLATING $B$ DECAYS

After getting constraints on new parameters such as leptoquark couplings and vector-like fermions masses, we now look for its implication on the rare lepton flavor violating (LFV)  $B$  decay modes.

The LFV  $B$  meson decays mediated by the  $b \rightarrow sl_i l_j$  quark level transitions are suppressed in the SM. However, it can be studied in the presence of SLQ. The one loop box diagram for  $b \rightarrow sl_i l_j$  processes mediated via the SLQ and vector-like fermions is presented in Fig. 7. In the presence of NP, the effective Hamiltonian for  $b \rightarrow sl_i^- l_j^+$  processes is given by

$$\mathcal{H}_{\text{eff}}(b \rightarrow sl_i^- l_j^+) = -\frac{G_F \alpha_{\text{em}}}{\sqrt{2}\pi} V_{tb} V_{ts}^* \left[ C_9^{\text{NP}} (\bar{s} \gamma^\mu P_L b) (\bar{l}_i \gamma_\mu l_j) + C_{10}^{\text{NP}} (\bar{s} \gamma^\mu P_L b) (\bar{l}_i \gamma_\mu \gamma_5 l_j) \right], \quad (47)$$

where  $C_{9,10}^{\text{NP}}$  are defined in Eqn. 12.

### A. $B_s \rightarrow l_i^- l_j^+$

The branching ratio of the LFV  $B_s \rightarrow l_i^- l_j^+$  decay process is given as [121]

$$\begin{aligned} \text{Br}(B_s \rightarrow l_i^- l_j^+) &= \tau_{B_s} \frac{\alpha_{\text{em}}^2 G_F^2}{64\pi^3 M_{B_s}^3} f_{B_s}^3 |V_{tb} V_{ts}^*|^2 \lambda^{1/2}(M_{B_s}, m_i, m_j) \\ &\times \left[ [M_{B_s}^2 - (m_i + m_j)^2](m_i - m_j)^2 |C_9^{\text{NP}}|^2 + [M_{B_s}^2 - (m_i - m_j)^2](m_i + m_j)^2 |C_{10}^{\text{NP}}|^2 \right]. \quad (48) \end{aligned}$$

### B. $B \rightarrow K l_i^- l_j^+$

The differential branching ratio of  $\bar{B} \rightarrow \bar{K} l_i^- l_j^+$  process is given as [69]

$$\frac{d\text{Br}}{dq^2}(\bar{B} \rightarrow \bar{K} l_i^- l_j^+) = \tau_B \frac{G_F^2 \alpha_{\text{em}}^2}{2^{12} \pi^5 M_B^3} \beta_{ij} \sqrt{\lambda(M_B^2, M_K^2, q^2)} |V_{tb} V_{ts}^*|^2 (J_1 + J_2), \quad (49)$$

where

$$\begin{aligned} J_1 &= 4 \left[ \left( 1 - \frac{(m_i - m_j)^2}{q^2} \right) \frac{1}{3} (2q^2 + (m_i + m_j)^2) |H_V^0|^2 \right. \\ &\quad \left. + \frac{(m_i - m_j)^2}{q^2} (q^2 - (m_i + m_j)^2) |H_V^t|^2 \right], \\ J_2 &= 4 \left[ \left( 1 - \frac{(m_i + m_j)^2}{q^2} \right) \frac{1}{3} (2q^2 + (m_i - m_j)^2) |H_A^0|^2 \right. \\ &\quad \left. + \frac{(m_i + m_j)^2}{q^2} (q^2 - (m_i - m_j)^2) |H_A^t|^2 \right], \quad (50) \end{aligned}$$

with

$$\begin{aligned}
H_V^0 &= \sqrt{\frac{\lambda(M_B^2, M_K^2, q^2)}{q^2}} f_+(q^2) C_9^{\text{NP}}, & H_V^t &= \frac{M_B^2 - M_K^2}{\sqrt{q^2}} f_0(q^2) C_9^{\text{NP}}, \\
H_A^0 &= \sqrt{\frac{\lambda(M_B^2, M_K^2, q^2)}{q^2}} f_+(q^2) C_{10}^{\text{NP}}, & H_A^t &= \frac{M_B^2 - M_K^2}{\sqrt{q^2}} f_0(q^2) C_{10}^{\text{NP}},
\end{aligned} \tag{51}$$

and

$$\beta_{ij} = \sqrt{\left(1 - \frac{(m_i + m_j)^2}{q^2}\right) \left(1 - \frac{(m_i - m_j)^2}{q^2}\right)}. \tag{52}$$

### C. $B \rightarrow K^* l_i^- l_j^+$ and $B_s \rightarrow \phi l_i^- l_j^+$

The differential branching ratio of  $\bar{B} \rightarrow \bar{K}^* l_i^- l_j^+$  decay process in the presence of SLQ and vector-like fermions is given by [121]

$$\frac{\text{dBr}}{\text{d}q^2}(\bar{B} \rightarrow \bar{K}^* l_i^- l_j^+) = \frac{1}{4} [3I_1^c(q^2) + 6I_1^s(q^2) - I_2^c(q^2) - 2I_2^s(q^2)], \tag{53}$$

where the angular coefficients  $I_i(q^2)$  are given by [122]

$$\begin{aligned}
I_1^s(q^2) &= [ |A_\perp^L|^2 + |A_\parallel|^2 + (L \rightarrow R) ] \frac{\lambda_q + 2[q^4 - (m_i^2 - m_j^2)^2]}{4q^4} + \frac{4m_i m_j}{q^2} \text{Re}(A_\parallel^L A_\parallel^{R*} + A_\perp^L A_\perp^{R*}), \\
I_1^c(q^2) &= [ |A_0^L|^2 + |A_0^R|^2 ] \frac{q^4 - (m_i^2 - m_j^2)^2}{q^4} + \frac{8m_i m_j}{q^2} \text{Re}(A_0^L A_0^{R*} - A_t^L A_t^{R*}) \\
&\quad - 2 \frac{(m_i^2 - m_j^2)^2 - q^2(m_i^2 + m_j^2)}{q^4} (|A_t^L|^2 + |A_t^R|^2), \\
I_2^s(q^2) &= \frac{\lambda_q}{4q^4} [ |A_\perp^L|^2 + |A_\parallel|^2 + (L \rightarrow R) ], \\
I_2^c(q^2) &= -\frac{\lambda_q}{q^4} (|A_0^L|^2 + |A_0^R|^2),
\end{aligned} \tag{54}$$

with the transversity amplitudes in terms of form factors and new Wilson coefficients are given as [122]

$$\begin{aligned}
A_\perp^{L(R)} &= N_{K^*} \sqrt{2} \lambda_B^{1/2} \left[ (C_9^{\text{NP}} \mp C_{10}^{\text{NP}}) \frac{V(q^2)}{M_B + M_{K^*}} \right], \\
A_\parallel^{L(R)} &= -N_{K^*} \sqrt{2} (M_B^2 - M_{K^*}^2) \left[ (C_9^{\text{NP}} \mp C_{10}^{\text{NP}}) \frac{A_1(q^2)}{M_B - M_{K^*}} \right], \\
A_0^{L(R)} &= -\frac{N_{K^*}}{2M_{K^*} \sqrt{q^2}} (C_9^{\text{NP}} \mp C_{10}^{\text{NP}}) \left( (M_B^2 - M_{K^*}^2 - q^2)(M_B + M_{K^*}) A_1(q^2) - \frac{\lambda_B A_2(q^2)}{M_B + M_{K^*}} \right), \\
A_t^{L(R)} &= -N_{K^*} \frac{\lambda_B^{1/2}}{\sqrt{q^2}} (C_9^{\text{NP}} \mp C_{10}^{\text{NP}}) A_0(q^2),
\end{aligned} \tag{55}$$

and

$$\lambda_B = \lambda(M_B^2, M_{K^*}^2, q^2), \quad \lambda_q = \lambda(m_i^2, m_j^2, q^2),$$

$$N_{K^*}(q^2) = V_{tb}V_{ts}^* \left[ \tau_{B_d} \frac{\alpha_{\text{em}}^2 G_F^2}{3 \times 2^{10} \pi^5 M_B^3} \lambda_B^{1/2} \lambda_q^{1/2} \right]^{1/2}. \quad (56)$$

After collecting the expressions for the LFV  $B_{(s)}$  meson decay modes, we now proceed for the numerical estimation. We have taken the lifetime of  $B_{(s)}$  meson, all the particles mass, the CKM matrix elements from PDG [103],  $B \rightarrow K$  form factor from [123],  $B_{(s)} \rightarrow (K^*, \phi)$  form factor from [107, 124]. Using the upper limit of the allowed parameter space from Table II, the leptoquark mass as  $M_{S_1} = 1200$  GeV, and the vector-like fermion masses as  $M_{\psi_q} = M_{N_1} = 820$  GeV,  $M_{N_2} = 800$  GeV, we have predicted the branching ratios of  $B_s \rightarrow \mu^- \tau^+ / \tau^- \mu^+$ ,  $B^{+(0)} \rightarrow K^{+(0)} \mu^- \tau^+ / \tau^- \mu^+$ ,  $B^{+(0)} \rightarrow K^{*+(0)} \mu^- \tau^+ / \tau^- \mu^+$  and  $B_s \rightarrow \phi \mu^- \tau^+ / \tau^- \mu^+$  processes, which are tabulated in Table III.

Decay modes	Predicted branching ratios	Experimental Limits (90% CL)
$B_s \rightarrow \mu^- \tau^+ / \mu^+ \tau^-$	$5.373 \times 10^{-8}$	$< 3.4 \times 10^{-5}$ [125]
$B^+ \rightarrow K^+ \mu^- \tau^+ / \mu^+ \tau^-$	$2.0 \times 10^{-7}$	$< 2.8 \times 10^{-5} / < 4.5 \times 10^{-5}$ [126]
$\bar{B}^0 \rightarrow \bar{K}^0 \mu^- \tau^+ / \mu^+ \tau^-$	$1.85 \times 10^{-7}$	...
$B^+ \rightarrow K^{*+} \mu^- \tau^+ / \mu^+ \tau^-$	$2.971 \times 10^{-7}$	...
$\bar{B}^0 \rightarrow \bar{K}^{*0} \mu^- \tau^+ / \mu^+ \tau^-$	$2.742 \times 10^{-7}$	...
$B_s \rightarrow \phi \mu^- \tau^+ / \mu^+ \tau^-$	$3.592 \times 10^{-7}$	...

TABLE III: Predicted branching ratios of lepton flavor violating decay modes of  $B_{(s)}$  meson.

Though the experimental limits on most of these decay modes are not yet available, from the table, one can notice that the branching ratios of the LFV  $B$  decay modes are within the reach of LHCb or  $B$  factories. There exist upper limit on only  $B_s \rightarrow \tau^\pm \mu^\mp$  [125] and  $B^+ \rightarrow K^+ \mu^- \tau^+ (\mu^+ \tau^-)$  [126] decay processes, for which our predicted branching ratios are well below the current 90% CL experimental upper limits. Using the above mentioned allowed parameter space, our predictions on the branching ratio of  $B_s \rightarrow \tau^\pm \mu^\mp$  process are

$$\text{Br}(B_s \rightarrow \tau^\pm \mu^\mp) = \text{Br}(B_s \rightarrow \tau^+ \mu^-) + \text{Br}(B_s \rightarrow \tau^- \mu^+) = 1.075 \times 10^{-7}, \quad (57)$$

within the current experimental limit at 90% C.L. [125]

$$\text{Br}(B_s \rightarrow \tau^\pm \mu^\mp)|^{\text{Exp}} < 3.4 \times 10^{-5}. \quad (58)$$

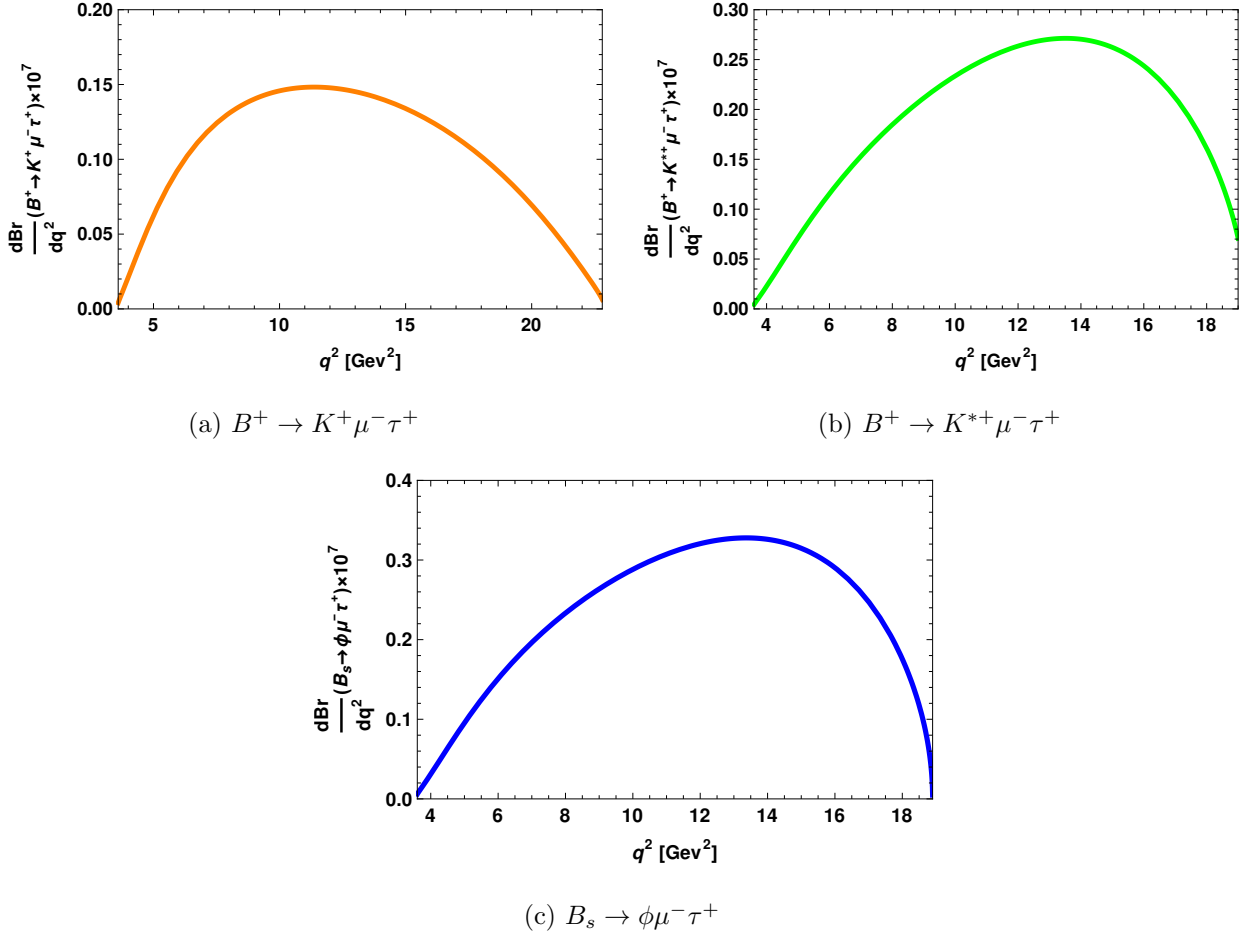


FIG. 12: The  $q^2$  variation of branching ratios of  $B^+ \rightarrow K^+ \mu^- \tau^+$  (top-left panel),  $B^+ \rightarrow K^{*+} \mu^- \tau^+$  (top-right panel) and  $B_s \rightarrow \phi \mu^- \tau^+$  (bottom panel) processes.

Fig. 12 depicts the branching ratios of  $B^+ \rightarrow K^+ \mu^- \tau^+$  (top-left panel),  $B^+ \rightarrow K^{*+} \mu^- \tau^+$  (top-right panel) and  $B_s \rightarrow \phi \mu^- \tau^+$  (bottom panel) LFV channels with respect to  $q^2$ .

## VII. COMMENTS ON NEUTRINO MASS

To realize neutrino mass, the model can be supplemented with three right-handed neutrinos ( $i = 3$ ) and allowing the Dirac interaction  $y_\nu^i \bar{\ell}_L \tilde{H} \xi_{iR}$ . Thus type-I seesaw provides  $m_\nu \sim (y_\nu^i v)^2 / M_{\xi_i}$ . For a sample case,  $M_{\xi_i} \sim 10$  TeV and  $y_\nu^i \sim 10^{-5}$  gives sub-eV scale neutrino mass and also doesn't alter the phenomenological aspects discussed earlier in the paper.

## VIII. CONCLUDING REMARKS

The model is motivated to shed light on dark matter and also the existing anomalies in flavor sector, associated with  $B$ -meson. For the purpose, we extend standard model with vector-like fermions of quark and lepton type. Aided with a  $(\bar{3}, 1, 1/3)$  scalar leptoquark, we build a platform for new physics in flavor sector. An admixture of neutral vector-like lepton constitutes the relic density of the Universe through annihilation and co-annihilation channels mediated via scalar bosons, gauge bosons and vector-like fermions, leading to a freeze-out scenario. Apart from, the spin independent WIMP-nucleon cross section via  $Z$ -portal dictates the amount of mixing in neutral vector-like leptons, and leptoquark-portal severely constrains the relevant Yukawa. Further, electroweak precision parameters constrain the mass splitting between the neutral vector-like components, to be above  $\sim 7$  GeV. In the presence of new vector-like fermions and scalar leptoquark, the rare  $b \rightarrow s$  transitions occur through one loop box diagrams. By using the recent measurements on the branching ratios of  $b \rightarrow sll(\nu_l\bar{\nu}_l)$  and  $b \rightarrow s\gamma$  processes such as  $B_s \rightarrow ll$ ,  $B \rightarrow K^{(*)}ll(\nu_l\bar{\nu}_l)$ ,  $\bar{B} \rightarrow X_s\gamma$ , and the lepton non-universality  $R_{K^{(*)}}$  observables, we further constrained the new parameters like leptoquark couplings, vector-like fermions masses and couplings. We then estimate the branching ratios of rare (semi)leptonic  $B_{(s)}$  decay modes which are found to be within the reach of Belle II and LHCb experiments.

### Acknowledgments

SS and RM would like to acknowledge University of Hyderabad IoE project grant no. RC1-20-012. RM acknowledges the support from SERB, Government of India, through grant No. EMR/2017/001448.

### Appendix A: Expressions of electroweak precision parameters

The interaction of gauge interaction of vector-like fermions, written in a general form as

$$\mathcal{L} \supset \bar{\psi}_a(g_V\gamma^\mu + g_A\gamma^\mu\gamma_5)\psi_b V_\mu. \quad (\text{A1})$$

Now, the electroweak parameters can be written in terms of  $\Pi$  function as

$$\Pi(q^2) = \frac{N_c}{4\pi^2} \left[ (g_V^2 + g_A^2)\tilde{\Pi}_{V+A}(q^2) + (g_V^2 - g_A^2)\tilde{\Pi}_{V-A}(q^2) \right], \quad (\text{A2})$$



where,  $N_c$  denotes the color charge of vector-like fermion. The expression for  $\Pi$  functions and their derivatives at  $q^2 = 0$  are given by [98]

$$\begin{aligned}\tilde{\Pi}_{V+A}(0) &= -\frac{(m_a^2 + m_b^2)}{2} \left( \text{Div} + \ln \left( \frac{\mu^2}{m_a m_b} \right) \right) - \frac{(m_a^2 + m_b^2)}{4} - \frac{(m_a^4 + m_b^4)}{4(m_a^2 - m_b^2)} \ln \left( \frac{m_b^2}{m_a^2} \right), \\ \tilde{\Pi}_{V-A}(0) &= m_a m_b \left( \text{Div} + \ln \left( \frac{\mu^2}{m_a m_b} \right) + \frac{(m_a^2 + m_b^2)}{2(m_a^2 - m_b^2)} \ln \left( \frac{m_b^2}{m_a^2} \right) + 1 \right),\end{aligned}\quad (\text{A3})$$

and the derivatives

$$\begin{aligned}\tilde{\Pi}'_{V+A}(0) &= \frac{1}{3} \text{Div} + \ln \left( \frac{\mu^2}{m_a m_b} \right) + \frac{(m_a^4 - 8m_a^2 m_b^2 + m_b^4)}{9(m_a^2 - m_b^2)^2} + \frac{(m_a^2 + m_b^2)(m_a^4 - 4m_a^2 m_b^2 + m_b^4)}{6(m_a^2 - m_b^2)^3} \ln \left( \frac{m_b^2}{m_a^2} \right), \\ \tilde{\Pi}'_{V-A}(0) &= \frac{m_a m_b (m_a^2 + m_b^2)}{2(m_a^2 - m_b^2)^2} + \frac{m_a^3 m_b^3}{(m_a^2 - m_b^2)^3} \ln \left( \frac{m_b^2}{m_a^2} \right).\end{aligned}\quad (\text{A4})$$

and

$$\begin{aligned}\tilde{\Pi}''_{V+A}(0) &= \frac{(m_a^2 + m_b^2)(m_a^4 - 8m_a^2 m_b^2 + m_b^4)}{4(m_a^2 - m_b^2)^4} - \frac{3m_a^4 m_b^4}{(m_a^2 - m_b^2)^5} \ln \left( \frac{m_b^2}{m_a^2} \right), \\ \tilde{\Pi}''_{V-A}(0) &= \frac{m_a m_b (m_a^4 + 10m_a^2 m_b^2 + m_b^4)}{3(m_a^2 - m_b^2)^4} + \frac{2(m_a^2 + m_b^2)m_a^3 m_b^3}{2(m_a^2 - m_b^2)^5} \ln \left( \frac{m_b^2}{m_a^2} \right).\end{aligned}\quad (\text{A5})$$

For identical masses i.e.,  $m_a = m_b$ , the above functions take the form

$$\begin{aligned}\tilde{\Pi}_{V+A}(0) &= -m_a^2 \text{Div} - m_a^2 \ln \left( \frac{\mu^2}{m_a^2} \right), \\ \tilde{\Pi}_{V-A}(0) &= m_a^2 \text{Div} + m_a^2 \ln \left( \frac{\mu^2}{m_a^2} \right), \\ \tilde{\Pi}'_{V+A}(0) &= \frac{1}{3} \text{Div} + \frac{1}{3} \ln \left( \frac{\mu^2}{m_a^2} \right) - \frac{1}{6}, \\ \tilde{\Pi}'_{V-A}(0) &= \frac{1}{6}, \\ \tilde{\Pi}''_{V+A}(0) &= \frac{1}{10m_a^2}, \\ \tilde{\Pi}''_{V-A}(0) &= \frac{1}{30m_a^2}.\end{aligned}\quad (\text{A6})$$

## Appendix B: $J_{1,2}^{s(c)}$ functions of $B \rightarrow K^* l^+ l^-$ process

The  $J_{1,2}^{s(c)}$  functions required to compute the decay rate of  $B \rightarrow K^* l l$  processes are given by [105]

$$J_1^s = \frac{(2 + \beta_l^2)}{4} \left[ |A_\perp^L|^2 + |A_\parallel^L|^2 + (L \rightarrow R) \right] + \frac{4m_l^2}{q^2} \text{Re} (A_\perp^L A_\perp^{R*} + A_\parallel^L A_\parallel^{R*}), \quad (\text{B1})$$

$$J_1^c = |A_0^L|^2 + |A_0^R|^2 + \frac{4m_l^2}{q^2} \left[ |A_t|^2 + 2\text{Re} (A_0^L A_0^{R*}) \right], \quad (\text{B2})$$

$$J_2^s = \frac{\beta_l^2}{4} [|A_\perp^L|^2 + |A_\parallel^L|^2 + (L \rightarrow R)], \quad (\text{B3})$$

$$J_2^c = -\beta_l^2 [|A_0^L|^2 + (L \rightarrow R)], \quad (\text{B4})$$

$$(\text{B5})$$

with

$$A_i A_j^* = A_i^L(q^2) A_j^{*L}(q^2) + A_i^R(q^2) A_j^{*R}(q^2) \quad (i, j = 0, \parallel, \perp), \quad (\text{B6})$$

in shorthand notation.

## Appendix C: Loop functions of muon anomalous magnetic moment

The loop functions involved in the scalar leptoquark contribution to muon anomalous magnetic moment are given as [127]

$$f_1(x_F) = m_1 \left( c_1 + \frac{3}{2} d_1 \right), \quad \bar{f}_1(x_F) = m_1 \left( -\bar{c}_1 + \frac{3}{2} \bar{d}_1 \right), \quad (\text{C1})$$

$$f_2(x_F) = m_2 \left( c_2 + \frac{3}{2} d_2 \right), \quad \bar{f}_2(x_F) = m_2 \left( -\bar{c}_2 + \frac{3}{2} \bar{d}_2 \right), \quad (\text{C2})$$

where

$$c = \frac{x_F - 3}{4(x_F - 1)^2} + \frac{\log x_F}{(x_F - 1)^3}, \quad d = \frac{-2x_F^2 + 7x_F - 11}{18(x_F - 1)^3} + \frac{\log x_F}{3(x_F - 1)^4}, \quad (\text{C3})$$

$$\bar{c} = \frac{3x_F - 1}{4(x_F - 1)^2} + \frac{x_F^2 \log x_F}{2(x_F - 1)^3}, \quad \bar{d} = \frac{11x_F^2 - 7x_F + 2}{18(x_F - 1)^3} - \frac{x_F^3 \log x_F}{3(x_F - 1)^4}. \quad (\text{C4})$$

---

[1] R. Aaij et al. (LHCb), Phys. Rev. Lett. **113**, 151601 (2014), 1406.6482.

- [2] R. Aaij et al. (LHCb) (2019), 1903.09252.
- [3] R. Aaij et al. (LHCb), JHEP **08**, 055 (2017), 1705.05802.
- [4] A. Abdesselam et al. (Belle) (2019), 1904.02440.
- [5] M. Huschle et al. (Belle), Phys. Rev. **D92**, 072014 (2015), 1507.03233.
- [6] A. Abdesselam et al. (Belle), in *Proceedings, 51st Rencontres de Moriond on Electroweak Interactions and Unified Theories: La Thuile, Italy, March 12-19, 2016* (2016), 1603.06711, URL <http://inspirehep.net/record/1431982/files/arXiv:1603.06711.pdf>.
- [7] A. Abdesselam et al. (2016), 1608.06391.
- [8] S. Hirose et al. (Belle), Phys. Rev. **D97**, 012004 (2018), 1709.00129.
- [9] S. Hirose et al. (Belle), Phys. Rev. Lett. **118**, 211801 (2017), 1612.00529.
- [10] R. Aaij et al. (LHCb), Phys. Rev. Lett. **120**, 121801 (2018), 1711.05623.
- [11] R. Aaij et al. (LHCb), Phys. Rev. Lett. **115**, 111803 (2015), [Erratum: Phys. Rev. Lett.115,no.15,159901(2015)], 1506.08614.
- [12] R. Aaij et al. (LHCb), Phys. Rev. **D97**, 072013 (2018), 1711.02505.
- [13] R. Aaij et al. (LHCb), Phys. Rev. Lett. **120**, 171802 (2018), 1708.08856.
- [14] J. P. Lees et al. (BaBar), Phys. Rev. Lett. **109**, 101802 (2012), 1205.5442.
- [15] J. P. Lees et al. (BaBar), Phys. Rev. **D88**, 072012 (2013), 1303.0571.
- [16] Heavy Flavor Averaging Group (2019), URL <https://hflav-eos.web.cern.ch/hflav-eos/semi/spring19/html/RDsDsstar/RDRDs.html>.
- [17] R. Aaij et al. (LHCb) (2021), 2103.11769.
- [18] C. Bobeth, G. Hiller, and G. Piranishvili, JHEP **12**, 040 (2007), 0709.4174.
- [19] M. Bordone, G. Isidori, and A. Pattori, Eur. Phys. J. **C76**, 440 (2016), 1605.07633.
- [20] B. Capdevila, A. Crivellin, S. Descotes-Genon, J. Matias, and J. Virto, JHEP **01**, 093 (2018), 1704.05340.
- [21] Y. S. Amhis et al. (HFLAV) (2019), 1909.12524, URL <https://hflav.web.cern.ch>.
- [22] H. Na, C. M. Bouchard, G. P. Lepage, C. Monahan, and J. Shigemitsu (HPQCD), Phys. Rev. **D92**, 054510 (2015), [Erratum: Phys. Rev.D93,no.11,119906(2016)], 1505.03925.
- [23] S. Fajfer, J. F. Kamenik, and I. Nisandzic, Phys. Rev. **D85**, 094025 (2012), 1203.2654.
- [24] S. Fajfer, J. F. Kamenik, I. Nisandzic, and J. Zupan, Phys. Rev. Lett. **109**, 161801 (2012), 1206.1872.
- [25] W.-F. Wang, Y.-Y. Fan, and Z.-J. Xiao, Chin. Phys. **C37**, 093102 (2013), 1212.5903.

- [26] M. A. Ivanov, J. G. Korner, and P. Santorelli, Phys. Rev. **D71**, 094006 (2005), [Erratum: Phys. Rev.D75,019901(2007)], hep-ph/0501051.
- [27] H. Georgi and S. L. Glashow, Phys. Rev. Lett. **32**, 438 (1974).
- [28] H. Georgi, AIP Conf. Proc. **23**, 575 (1975).
- [29] H. Fritzsch and P. Minkowski, Annals Phys. **93**, 193 (1975).
- [30] P. Langacker, Phys. Rept. **72**, 185 (1981).
- [31] J. C. Pati and A. Salam, Phys. Rev. **D10**, 275 (1974), [Erratum: Phys. Rev.D11,703(1975)].
- [32] J. C. Pati and A. Salam, Phys. Rev. **D8**, 1240 (1973).
- [33] J. C. Pati and A. Salam, Phys. Rev. Lett. **31**, 661 (1973).
- [34] O. U. Shanker, Nucl. Phys. **B206**, 253 (1982).
- [35] O. U. Shanker, Nucl. Phys. **B204**, 375 (1982).
- [36] B. Gripaios, JHEP **02**, 045 (2010), 0910.1789.
- [37] B. Schrempp and F. Schrempp, Phys. Lett. **153B**, 101 (1985).
- [38] D. B. Kaplan, Nucl. Phys. **B365**, 259 (1991).
- [39] A. K. Alok, B. Bhattacharya, A. Datta, D. Kumar, J. Kumar, and D. London, Phys. Rev. **D96**, 095009 (2017), 1704.07397.
- [40] D. Bećirević and O. Sumensari, JHEP **08**, 104 (2017), 1704.05835.
- [41] G. Hiller and I. Nisandzic, Phys. Rev. **D96**, 035003 (2017), 1704.05444.
- [42] G. D'Amico, M. Nardecchia, P. Panci, F. Sannino, A. Strumia, R. Torre, and A. Urbano, JHEP **09**, 010 (2017), 1704.05438.
- [43] D. Bećirević, S. Fajfer, N. Košnik, and O. Sumensari, Phys. Rev. **D94**, 115021 (2016), 1608.08501.
- [44] M. Bauer and M. Neubert, Phys. Rev. Lett. **116**, 141802 (2016), 1511.01900.
- [45] L. Calibbi, A. Crivellin, and T. Ota, Phys. Rev. Lett. **115**, 181801 (2015), 1506.02661.
- [46] M. Freytsis, Z. Ligeti, and J. T. Ruderman, Phys. Rev. **D92**, 054018 (2015), 1506.08896.
- [47] B. Dumont, K. Nishiwaki, and R. Watanabe, Phys. Rev. **D94**, 034001 (2016), 1603.05248.
- [48] I. Doršner, S. Fajfer, A. Greljo, J. F. Kamenik, and N. Košnik, Phys. Rept. **641**, 1 (2016), 1603.04993.
- [49] I. de Medeiros Varzielas and G. Hiller, JHEP **06**, 072 (2015), 1503.01084.
- [50] I. Dorsner, J. Drobnak, S. Fajfer, J. F. Kamenik, and N. Kosnik, JHEP **11**, 002 (2011), 1107.5393.

- [51] S. Davidson, D. C. Bailey, and B. A. Campbell, *Z. Phys.* **C61**, 613 (1994), hep-ph/9309310.
- [52] J. P. Saha, B. Misra, and A. Kundu, *Phys. Rev.* **D81**, 095011 (2010), 1003.1384.
- [53] R. Mohanta, *Phys. Rev.* **D89**, 014020 (2014), 1310.0713.
- [54] S. Sahoo and R. Mohanta, *New J. Phys.* **18**, 013032 (2016), 1509.06248.
- [55] S. Sahoo and R. Mohanta, *Phys. Rev.* **D93**, 114001 (2016), 1512.04657.
- [56] S. Sahoo and R. Mohanta, *Phys. Rev.* **D93**, 034018 (2016), 1507.02070.
- [57] S. Sahoo and R. Mohanta, *Phys. Rev.* **D91**, 094019 (2015), 1501.05193.
- [58] N. Kosnik, *Phys. Rev.* **D86**, 055004 (2012), 1206.2970.
- [59] S. Singirala, S. Sahoo, and R. Mohanta, *Phys. Rev. D* **99**, 035042 (2019), 1809.03213.
- [60] B. Chauhan, B. Kindra, and A. Narang, *Phys. Rev.* **D97**, 095007 (2018), 1706.04598.
- [61] D. Bečirević, I. Doršner, S. Fajfer, N. Košnik, D. A. Faroughy, and O. Sumensari, *Phys. Rev.* **D98**, 055003 (2018), 1806.05689.
- [62] A. Angelescu, D. Bečirević, D. A. Faroughy, and O. Sumensari, *JHEP* **10**, 183 (2018), 1808.08179.
- [63] S. Sahoo and R. Mohanta, *Eur. Phys. J. C* **77**, 344 (2017), 1705.02251.
- [64] S. Sahoo and R. Mohanta, *New J. Phys.* **18**, 093051 (2016), 1607.04449.
- [65] S. Sahoo and R. Mohanta, *J. Phys. G* **44**, 035001 (2017), 1612.02543.
- [66] S. Sahoo and A. Bhol (2020), 2005.12630.
- [67] A. Bhol, S. Sahoo, and S. R. Singh (2021), 2106.06155.
- [68] S. Singirala, S. Sahoo, and R. Mohanta (2021), 2106.03735.
- [69] M. Duraisamy, S. Sahoo, and R. Mohanta, *Phys. Rev. D* **95**, 035022 (2017), 1610.00902.
- [70] S. Sahoo, R. Mohanta, and A. K. Giri, *Phys. Rev. D* **95**, 035027 (2017), 1609.04367.
- [71] S. A. R. Ellis, R. M. Godbole, S. Gopalakrishna, and J. D. Wells, *JHEP* **09**, 130 (2014), 1404.4398.
- [72] N. Aghanim et al. (Planck) (2018), 1807.06209.
- [73] R. Mahbubani and L. Senatore, *Phys. Rev. D* **73**, 043510 (2006), hep-ph/0510064.
- [74] N. Arkani-Hamed, S. Dimopoulos, and S. Kachru (2005), hep-th/0501082.
- [75] F. D'Eramo, *Phys. Rev. D* **76**, 083522 (2007), 0705.4493.
- [76] R. Enberg, P. J. Fox, L. J. Hall, A. Y. Papaioannou, and M. Papucci, *JHEP* **11**, 014 (2007), 0706.0918.
- [77] T. Cohen, J. Kearney, A. Pierce, and D. Tucker-Smith, *Phys. Rev. D* **85**, 075003 (2012),

1109.2604.

- [78] C. Cheung and D. Sanford, *JCAP* **02**, 011 (2014), 1311.5896.
- [79] D. Restrepo, A. Rivera, M. Sánchez-Peláez, O. Zapata, and W. Tangarife, *Phys. Rev. D* **92**, 013005 (2015), 1504.07892.
- [80] L. Calibbi, A. Mariotti, and P. Tziveloglou, *JHEP* **10**, 116 (2015), 1505.03867.
- [81] G. Cynolter, J. Kovács, and E. Lendvai, *Mod. Phys. Lett. A* **31**, 1650013 (2016), 1509.05323.
- [82] S. Bhattacharya, N. Sahoo, and N. Sahu, *Phys. Rev. D* **93**, 115040 (2016), 1510.02760.
- [83] S. Bhattacharya, N. Sahoo, and N. Sahu, *Phys. Rev. D* **96**, 035010 (2017), 1704.03417.
- [84] S. Bhattacharya, P. Ghosh, N. Sahoo, and N. Sahu, *Front. in Phys.* **7**, 80 (2019), 1812.06505.
- [85] A. Freitas, S. Westhoff, and J. Zupan, *JHEP* **09**, 015 (2015), 1506.04149.
- [86] B. Barman, D. Borah, P. Ghosh, and A. K. Saha, *JHEP* **10**, 275 (2019), 1907.10071.
- [87] B. Barman, A. Dutta Banik, and A. Paul, *Phys. Rev. D* **101**, 055028 (2020), 1912.12899.
- [88] A. Dutta Banik, A. K. Saha, and A. Sil, *Phys. Rev. D* **98**, 075013 (2018), 1806.08080.
- [89] S. Bhattacharya, P. Ghosh, and N. Sahu, *JHEP* **02**, 059 (2019), 1809.07474.
- [90] B. Barman, S. Bhattacharya, P. Ghosh, S. Kadam, and N. Sahu, *Phys. Rev. D* **100**, 015027 (2019), 1902.01217.
- [91] A. V. Semenov (1996), hep-ph/9608488.
- [92] A. Pukhov, E. Boos, M. Dubinin, V. Edneral, V. Ilyin, D. Kovalenko, A. Kryukov, V. Savrin, S. Shichanin, and A. Semenov (1999), hep-ph/9908288.
- [93] G. Belanger, F. Boudjema, A. Pukhov, and A. Semenov, *Comput. Phys. Commun.* **176**, 367 (2007), hep-ph/0607059.
- [94] G. Belanger, F. Boudjema, A. Pukhov, and A. Semenov, *Comput. Phys. Commun.* **180**, 747 (2009), 0803.2360.
- [95] P. Agrawal, Z. Chacko, C. Kilic, and R. K. Mishra (2010), 1003.1912.
- [96] E. Aprile et al. (XENON), *Phys. Rev. Lett.* **121**, 111302 (2018), 1805.12562.
- [97] C. Amole et al. (PICO), *Phys. Rev. D* **100**, 022001 (2019), 1902.04031.
- [98] G. Cynolter and E. Lendvai, *Eur. Phys. J. C* **58**, 463 (2008), 0804.4080.
- [99] R. Barbieri, A. Pomarol, R. Rattazzi, and A. Strumia, *Nucl. Phys. B* **703**, 127 (2004), hep-ph/0405040.
- [100] C. Bobeth, M. Misiak, and J. Urban, *Nucl. Phys.* **B574**, 291 (2000), hep-ph/9910220.
- [101] C. Bobeth, A. J. Buras, F. Kruger, and J. Urban, *Nucl. Phys.* **B630**, 87 (2002), hep-

ph/0112305.

- [102] W.-S. Hou, M. Kohda, and F. Xu, Phys. Rev. **D90**, 013002 (2014), 1403.7410.
- [103] P. A. Zyla et al. (Particle Data Group), PTEP **2020**, 083C01 (2020).
- [104] P. Colangelo, F. De Fazio, P. Santorelli, and E. Scrimieri, Phys. Lett. **B395**, 339 (1997), hep-ph/9610297.
- [105] C. Bobeth, G. Hiller, and G. Piranishvili, JHEP **07**, 106 (2008), 0805.2525.
- [106] W. Altmannshofer, P. Ball, A. Bharucha, A. J. Buras, D. M. Straub, and M. Wick, JHEP **01**, 019 (2009), 0811.1214.
- [107] P. Ball and R. Zwicky, Phys. Rev. D **71**, 014029 (2005), hep-ph/0412079.
- [108] A. Abdesselam et al. (Belle) (2019), 1908.01848.
- [109] A. J. Buras, J. Girrbach-Noe, C. Niehoff, and D. M. Straub, JHEP **02**, 184 (2015), 1409.4557.
- [110] Y. Sakaki, M. Tanaka, A. Tayduganov, and R. Watanabe, Phys. Rev. **D88**, 094012 (2013), 1309.0301.
- [111] A. J. Buras, in *Probing the standard model of particle interactions. Proceedings, Summer School in Theoretical Physics, NATO Advanced Study Institute, 68th session, Les Houches, France, July 28-September 5, 1997. Pt. 1, 2* (1998), pp. 281–539, hep-ph/9806471.
- [112] W. Altmannshofer, A. J. Buras, D. M. Straub, and M. Wick, JHEP **04**, 022 (2009), 0902.0160.
- [113] C. S. Kim, Y. G. Kim, and T. Morozumi, Phys. Rev. D **60**, 094007 (1999), hep-ph/9905528.
- [114] M. Misiak et al., Phys. Rev. Lett. **114**, 221801 (2015), 1503.01789.
- [115] Y. Amhis et al. (HFLAV), Eur. Phys. J. **C77**, 895 (2017), 1612.07233.
- [116] G. W. Bennett et al. (Muon g-2), Phys. Rev. **D73**, 072003 (2006), hep-ex/0602035.
- [117] T. Aoyama et al., Phys. Rept. **887**, 1 (2020), 2006.04822.
- [118] T. Blum, P. A. Boyle, V. Gülpers, T. Izubuchi, L. Jin, C. Jung, A. Jüttner, C. Lehner, A. Portelli, and J. T. Tsang (RBC, UKQCD), Phys. Rev. Lett. **121**, 022003 (2018), 1801.07224.
- [119] A. Keshavarzi, D. Nomura, and T. Teubner, Phys. Rev. D **97**, 114025 (2018), 1802.02995.
- [120] B. Abi et al. (Muon g-2), Phys. Rev. Lett. **126**, 141801 (2021), 2104.03281.
- [121] D. Bečirević, O. Sumensari, and R. Zukanovich Funchal, Eur. Phys. J. C **76**, 134 (2016), 1602.00881.
- [122] M. Nebot, J. F. Oliver, D. Palao, and A. Santamaria, Phys. Rev. D **77**, 093013 (2008), 0711.0483.

- [123] P. Ball and R. Zwicky, *Phys. Rev.* **D71**, 014015 (2005), hep-ph/0406232.
- [124] M. Beneke, T. Feldmann, and D. Seidel, *Eur. Phys. J. C* **41**, 173 (2005), hep-ph/0412400.
- [125] R. Aaij et al. (LHCb), *Phys. Rev. Lett.* **123**, 211801 (2019), 1905.06614.
- [126] J. P. Lees et al. (BaBar), *Phys. Rev. D* **86**, 012004 (2012), 1204.2852.
- [127] L. Lavoura, *Eur. Phys. J.* **C29**, 191 (2003), hep-ph/0302221.